

## Implications of $^{36}\text{Cl}$ exposure ages from Skye, northwest Scotland for the timing of ice stream deglaciation and deglacial ice dynamics

Small, David ; Rinterknecht, Vincent; Austin, William E.N.; Bates, Richard; Benn, Douglas I.; Scourse, James; Bourles, Didier L.; Hibbert, Fiona D.

### Quaternary Science Reviews

DOI:

[10.1016/j.quascirev.2016.08.028](https://doi.org/10.1016/j.quascirev.2016.08.028)

Published: 15/10/2016

Peer reviewed version

[Cyswllt i'r cyhoeddiad / Link to publication](#)

*Dyfyniad o'r fersiwn a gyhoeddwyd / Citation for published version (APA):*

Small, D., Rinterknecht, V., Austin, W. E. N., Bates, R., Benn, D. I., Scourse, J., Bourles, D. L., & Hibbert, F. D. (2016). Implications of  $^{36}\text{Cl}$  exposure ages from Skye, northwest Scotland for the timing of ice stream deglaciation and deglacial ice dynamics. *Quaternary Science Reviews*, 150, 130-145. <https://doi.org/10.1016/j.quascirev.2016.08.028>

### Hawliau Cyffredinol / General rights

Copyright and moral rights for the publications made accessible in the public portal are retained by the authors and/or other copyright owners and it is a condition of accessing publications that users recognise and abide by the legal requirements associated with these rights.

- Users may download and print one copy of any publication from the public portal for the purpose of private study or research.
- You may not further distribute the material or use it for any profit-making activity or commercial gain
- You may freely distribute the URL identifying the publication in the public portal ?

### Take down policy

If you believe that this document breaches copyright please contact us providing details, and we will remove access to the work immediately and investigate your claim.

Manuscript Number: JQSR-D-16-00230R1

Title: Implications of  $^{36}\text{Cl}$  exposure ages from Skye, northwest Scotland for the timing of ice stream deglaciation and deglacial ice dynamics.

Article Type: Research paper

Keywords: Deglaciation; Scotland; Cosmogenic exposure ages; Chlorine-36.

Corresponding Author: Dr. David Small, Ph.D

Corresponding Author's Institution: University of Glasgow

First Author: David Small, Ph.D

Order of Authors: David Small, Ph.D; Vincent Rinterknecht; William Austin; Richard Bates; Douglas I Benn; James D Scourse; Didier L Bourlès; Fiona D Hibbert

Abstract: Constraining the past response of marine terminating ice streams during episodes of deglaciation provides important insights into potential future changes due to climate change. This paper presents new  $^{36}\text{Cl}$  cosmic ray exposure dating from boulders located on two moraines (Glen Brittle and Loch Scavaig) in southern Skye, northwest Scotland. Ages from the Glen Brittle moraines constrain deglaciation of a major marine terminating ice stream, the Barra-Donegal Ice Stream that drained the former British-Irish Ice Sheet, depending on choice of production method and scaling model this occurred  $19.9 \pm 1.5 - 17.6 \pm 1.3$  ka ago. We compare this timing of deglaciation to existing geochronological data and changes in a variety of potential forcing factors constrained through proxy records and numerical models to determine what deglaciation age is most consistent with existing evidence. Another small section of moraine, the Scavaig moraine, is traced offshore through multibeam swath-bathymetry and interpreted as delimiting a later stillstand/readvance stage following ice stream deglaciation. Additional cosmic ray exposure dating from the onshore portion of this moraine indicate that it was deposited  $16.3 \pm 1.3 - 15.2 \pm 0.9$  ka ago. When calculated using the most up-to-date scaling scheme this time of deposition is, within uncertainty, the same as the timing of a widely identified readvance, the Wester Ross Readvance, observed elsewhere in northwest Scotland. This extends the area over which this readvance has potentially occurred, reinforcing the view that it was climatically forced.



University of  
St Andrews | FOUNDED  
1413 |

Department of Earth & Environmental Sciences

David Small  
Department of Geography and Earth Sciences  
University of Glasgow  
Glasgow, G12 8QQ  
Scotland  
12/08/2016

Dear Editor,

We would like the editor to consider our revised manuscript entitled “Implications of  $^{36}\text{Cl}$  exposure ages from Skye, northwest Scotland for the timing of ice stream deglaciation and deglacial ice dynamics.” for publication in *Quaternary Science Reviews*.

We have included a point-by-point response to the reviewers comments with this submission. As can be seen from this we have adopted the reviewers points in near entirety. Specifically we have added labels to ensure all place names are indicated on maps, or simplified the terminology accordingly. Additionally we have included two new figures which locate the sampled boulders more precisely and depict their geomorphological setting. The  $^{36}\text{Cl}$  age calculations have been checked, in conversation with Shasta Marrero and amended where they were incorrect, as suggested by a reviewer and communicated to us by the editor.

We would like to take this opportunity to thank editor for handling the reviewing process to date, and to thank the reviewers for their considered comments that have improved the manuscript.

Yours sincerely,

Dr. David Small (corresponding author)

**Implications of <sup>36</sup>Cl exposure ages from Skye, northwest Scotland for the timing of ice stream deglaciation and deglacial ice dynamics.**

David Small <sup>a\*, 1</sup>, Vincent Rinterknecht <sup>a, b</sup>, William E. N. Austin <sup>a, c</sup>, Richard Bates <sup>a</sup>, Douglas I. Benn <sup>a</sup>, James D. Scourse <sup>d</sup>, Didier L. Bourlès <sup>e</sup>, ASTER Team <sup>e, ±</sup>, Fiona D. Hibbert <sup>f</sup>

<sup>a</sup> School of Geography and Geosciences, University of St Andrews, St Andrews, KY16 9AL, UK.

<sup>b</sup> Université Paris 1 Panthéon-Sorbonne, CNRS Laboratoire de Géographie Physique, F-92195 Meudon, France.

<sup>c</sup> Scottish Marine Institute, Scottish Association for Marine Sciences, Oban, PA37 1QA, UK.

<sup>d</sup> School of Ocean Sciences, Bangor University, Menai Bridge, Anglesey, LL59 5AB, UK.

<sup>e</sup> Aix-Marseille Université, CNRS-IRD-Collège de France, UM 34 CEREGE, Technopôle de l'Environnement Arbois-Méditerranée, BP80, 13545 Aix-en-Provence, France.

<sup>e</sup> Research School of<sup>f</sup> Ocean and Earth Sciences, The Australian National University, Canberra, ACT 2601, Australia

<sup>1</sup> To whom correspondence should be addressed: [David.Small@glasgow.ac.uk](mailto:David.Small@glasgow.ac.uk)

\* Now at Department of Geographical and Earth Sciences, University of Glasgow, Glasgow, G12 8QQ, UK. +44 141 330 5442.

<sup>±</sup> Maurice Arnold, Georges Aumaître, Karim Keddadouche.

## **Abstract**

Geochronological constraints on the deglaciation of former marine based ice streams provide information on the rates and modes by which marine based ice sheets have responded to external forcing factors such as climate change. This paper presents new  $^{36}\text{Cl}$  cosmic ray exposure dating from boulders located on two moraines (Glen Brittle and Loch Scavaig) in southern Skye, northwest Scotland. Ages from the Glen Brittle moraines constrain deglaciation of a major marine terminating ice stream, the Barra-Donnegal Ice Stream that drained the former British-Irish Ice Sheet, depending on choice of production method and scaling model this occurred  $19.9 \pm 1.5 - 17.6 \pm 1.3$  ka ago. We compare this timing of deglaciation to existing geochronological data and changes in a variety of potential forcing factors constrained through proxy records and numerical models to determine what deglaciation age is most consistent with existing evidence. Another small section of moraine, the Scavaig moraine, is traced offshore through multibeam swath-bathymetry and interpreted as delimiting a later stillstand/readvance stage following ice stream deglaciation. Additional cosmic ray exposure dating from the onshore portion of this moraine indicate that it was deposited  $16.3 \pm 1.3 - 15.2 \pm 0.9$  ka ago. When calculated using the most up-to-date scaling scheme this time of deposition is, within uncertainty, the same as the timing of a widely identified readvance, the Wester Ross Readvance, observed elsewhere in northwest Scotland. This extends the area over which this readvance has potentially occurred, reinforcing the view that it was climatically forced.

## **1. Introduction**

Concerns over the stability of the remaining ice sheets have been raised by suggestions that irreversible collapse of some marine based sectors is possible or has already begun,

with attendant effects on associated terrestrial glaciers (Joughin et al., 2014; Wouters et al., 2015). Marine terminating ice streams are important components of the interconnected ocean-cryosphere system because they discharge large volumes of ice directly into the ocean through calving (Alley and MacAyeal, 1994; Bradwell and Stoker, 2015; Deschamps et al., 2012). While modern observations provide useful information, the temporal coverage is not sufficient to capture the complete response of a marine terminating ice stream to rapid climate change. Researchers are therefore increasingly drawn to analogous palaeo-settings where the complete deglaciation record can be observed (Serjup et al., 2000; Dowdeswell et al., 2014; Svendsen et al., 2015).

Of the Pleistocene ice sheets, the British-Irish Ice Sheet (BIIS) provides a useful analogue. Its western margin was marine terminating while its position next to a major surficial artery of the Atlantic Meridional Overturning Circulation (AMOC) rendered it potentially sensitive to small climatic perturbations (Knutz et al., 2007). This sensitivity is captured in proxy data (Scourse et al., 2009; Hibbert et al., 2010) and numerical modelling experiments (Hubbard et al., 2009). Past reconstructions of the BIIS relied heavily on onshore mapping of landforms that can be inferred to represent former ice limits including terminal, lateral and recessional moraines (Sissons et al., 1973; Ballantyne, 1989, Bennett and Boulton, 1993; Clark et al., 2004). Recent advances in offshore geomorphological mapping, particularly the use of bathymetric and seismic data, have allowed workers to identify sediments and landforms associated with ice extending onto the continental shelf (Bradwell et al., 2008a; Dunlop et al., 2010; Ó'Cofaigh et al., 2012). This has allowed delimitation of fast flowing ice streams that drained much of the western sector of the former BIIS (Scourse et al., 2000; Stoker and Bradwell, 2005; Howe et al., 2012; Bradwell and Stoker, 2015; Dove et al., 2015). Further identification of subsequent landforms associated with confined ice flow casts

light on post-ice streaming behaviour inshore of the onset zone of the BDIS (Howe et al., 2012; Dove et al., 2015).

The Barra-Donegal Ice Stream (BDIS) drained a large portion of the western BIIS and, at the Last Glacial Maximum (LGM), reached the shelf edge (Knutz et al., 2001) where it deposited glaciogenic sediments in the Barra-Donegal Fan (BDF), the southernmost glaciogenic fan on the Eurasian continental margin (Figure 1). Recent observations using swath bathymetry have revealed a suite of glaciogenic landforms at the bed of the former BDIS, stretching from Skye in the north to Islay in the south (Howe et al., 2012; Dove et al., 2015). The BDIS flowed southwest from the Inner Hebrides before turning west around the Outer Hebrides towards the outer shelf (Howe et al., 2012). Large scale erosional features such as glacially over-deepened basins and streamlined bedrock are observed across large areas of the BDIS and provide important information on past ice flow directions. In comparison, large moraines are confined to the mid-outer shelf with smaller recessional moraines being more abundant in the nearshore (Dunlop et al., 2010; Dove et al., 2015).

Offshore evidence from ice rafted detritus (IRD) demonstrates that ice sourced in Scotland reached the shelf edge by 29 ka with a significant reduction in IRD delivery after 23 ka (Knutz et al., 2001; Scourse et al., 2009; Hibbert et al., 2010). To the north, basal marine radiocarbon ages show deglaciation of mid-shelf (Figure 1; Table 1) prior to  $16.7 \pm 0.3$  ka (Peacock et al., 1992; Austin and Kroon, 1996; Small et al., 2013) while cosmogenic exposure and radiocarbon ages (Figure 1) show initial deglaciation of the southern sector of the BDIS before ~20.0 ka (McCabe et al., 2003; Clark et al., 2009). Complete deglaciation of the southern sector occurred before 16.8 ka (Figure 1) (Ballantyne et al., 2014), an inference supported by IRD evidence that the BIIS maintained calving margins throughout the period 23.0-16.0 ka (Scourse et al., 2009,

Small et al., 2013). All available geochronological data related to the BDIS was synthesised to produce 1 ka time-slices of the pattern of deglaciation (Clark et al., 2012), this was subsequently refined to include maximum and minimum ice-extents at the same temporal resolution (Hughes et al., 2016). In the BDIS sector both reconstructions depict initial deglaciation from the shelf edge at c.25 ka with ice persisting on the mid-shelf until 19-17 ka. Rapid deglaciation occurs 17-16 ka by which time the ice margin is located near the present day coastline (Figure 1).

While the submarine geomorphology and retreat pattern of the BDIS is relatively well established (Howe et al., 2012; Dove et al., 2015), post-ice streaming behaviour and geochronological data relating to deglaciation of the northern sector of the BDIS is still comparatively limited. In northwest Scotland a regional scale readvance, the Wester Ross readvance has been delimited from a suite of onshore moraines and dated with  $^{10}\text{Be}$  exposure ages to  $\sim 16$  ka (Robinson and Ballantyne, 1979; Bradwell et al., 2008; Ballantyne et al., 2009). However, to date this readvance has not been identified south of Skye. In this contribution we present bathymetric data from inshore waters near Skye, which highlights ice dynamics following ice stream retreat. Cosmogenic  $^{36}\text{Cl}$  cosmic ray exposure (CRE) ages from moraine boulders provide geochronological constraints on the timing of this deglaciation.

## 2. Study Site

Skye is located off the west coast of Scotland, >200 km upstream from the maximum extent of the BDIS at the shelf break (Figure 1). During the LGM the mountains of central Skye (the Cuillin) nourished an independent ice dome, the Skye Ice Dome (SID), which deflected ice moving from the mainland to the west and acted as an ice divide between the BDIS and the Minch Ice Stream (MIS). Together, these ice streams drained



the majority of the northern sector of the BDIS (Bradwell et al., 2008a). To the north of Skye, the zone of confluence between mainland ice and the SID is inferred to follow the narrow straits between Skye and the islands of Scalpay and Raasay (Harker, 1901) (Figure 2). To the south, mainland erratics occur on the island of Soay and the orientation of striae on the southern margin of the Cuillin suggest that locally nourished ice was strongly deflected westwards by mainland ice. This implies that the zone of ice confluence lay between Skye and the neighbouring island of Soay (Ballantyne et al., 1991). The southern branch of mainland ice, along with ice flowing south from the Cuillin, fed the embryonic BDIS with ice stream onset beyond Rum (Howe et al., 2012; Dove et al., 2015). The northern branch fed the MIS (Stoker and Bradwell, 2005). Given its central position within the BDIS, Skye is an important location for constraining deglaciation of the BDIS and comparing the deglacial history of neighbouring ice streams that drained a dynamic, marine-based ice sheet.

Deglaciation of the MIS is constrained by several CRE ages. Two  $^{36}\text{Cl}$  CRE ages from ice smoothed bedrock on a col in Trotternish (Figure 2) show deglaciation at altitude in Northern Skye before ~16 ka (Stone et al., 1998). Further constraint on final deglaciation of the MIS is provided by five  $^{10}\text{Be}$  CRE ages with a mean age of  $15.9 \pm 1.0$  ka from a boulder moraine at Strollamus (Small et al., 2012), above the strait that separates Skye from Scalpay (Figure 2). In contrast, the only CRE ages from southern Skye are from a moraine related to the later Loch Lomond Readvance (LLR) (Small et al., 2012).

Our study focuses on two locations in Southern Skye where there are moraines outside the well mapped LLR limits., Glen Brittle to the west of the Cuillin, and Loch Scavaig, to the south (Figures 2 and 5). At both sites the moraines represent the innermost pre-LLR limit yet identified but without geochronological control it is not

possible to determine if they were deposited contemporaneously. In lower Glen Brittle the up-valley termination of raised shorelines coincides with a series of low moraine ridges littered with basalt boulders which have been interpreted as terminal moraines (Walker *et al.*, 1988). These moraines occur well outside the mapped limits of the LLR (Ballantyne, 1989) and thus clearly pre-date them (Figure 3). In Glen Brittle there are two main parallel moraine ridges up to 100 m long and 2-3m high (Figure 3). The ridges are separated by ~50 m.

On Soay, which forms the western margin of Loch Scavaig, a small moraine section comes onshore at the northeastern corner of the island (Clough and Harker, 1904). This moraine section is ~200-300 m in length and 4-5 m high in places. Large erratic gabbro boulders are found on its crest indicating that at some time following deglaciation of the BDIS ice sourced from the Cuillin extended into Loch Scavaig and reached Soay which itself is composed entirely of Torridonian sandstone with some Tertiary basalt dykes (Clough and Harker, 1904).

### **3. Methods**

#### *3.1 Bathymetry*

To constrain deglaciation of the BDIS we confirmed the presence of ice margin positions in southern Skye from onshore fieldwork in Glen Brittle and a bathymetric survey of Loch Scavaig. This study used a SEA SwathPlus High Frequency System with a central frequency of 468 kHz and a ping rate of up to 30 pings per second giving a potential footprint of less than 5 cm at standard survey speed. Data were acquired with a TSSDMS205 motion reference unit and positioning provided by a Topcon Hiper RTK dGPS. The RTK dGPS base system was established on the loch shore and tied to the

BNG datum using Rinex corrections from the OS. An Applied Microsystems MicroSV sound velocity probe was mounted at the sonar head in order to record changes in velocity due to mixing of different waters (and thus potential salinity changes) in the relatively enclosed waters of the loch. Final data were recorded to a position accuracy of better than  $\pm 5$  cm, however the final data set was processed to a bin resolution of 2 m with vertical heights given to  $\pm 20$  cm. The data was processed using SwathPlus and GridProcessor (SEA Ltd) with further editing using IVS Fledermaus. Bathymetric data points were converted from WGS84 to OSGP using the OSGB36 datum (origin 49°N and 2°W). Final data processing was accomplished within ArcGIS (v10).

### 3.2 Surface exposure dating using $^{36}\text{Cl}$ .

#### 3.2.1 Sampling

Moraines with suitable material for CRE dating using *in situ*-produced cosmogenic  $^{36}\text{Cl}$  were identified in Glen Brittle and on the island of Soay where the onshore continuation of an offshore moraine is located. Eleven samples, four from Glen Brittle and seven from Soay, were collected from basic igneous boulders (basalt and gabbro) for CRE dating. In Glen Brittle two samples were collected from the outer moraine ridge (BRI01 and BRI04) and two samples from the inner moraine ridge (BRI02 and BRI03). On Soay seven samples were collected from the onshore moraine section (Figure 4).

We selected boulders from moraine crests with the largest *b*-axis to minimise the potential for disturbance and snow cover. Where possible we sampled sub-rounded boulders considered indicative of sub-glacial transport (Ballantyne and Stone, 2009) to minimise the potential for inheritance. Similarly we sampled boulders with intact top surfaces as they are least likely to have experienced significant chemical weathering and

to minimise the potential influence of spallation of material. Samples were collected from the top surfaces of boulders using hammer and chisel. When possible, we sampled flat surfaces but, where necessary, strike and dip were recorded using a compass-clinometer. Detailed site descriptions (e.g. geomorphological context, boulder dimensions, weathering) were made for each sample. Sample locations and elevations were recorded using a hand-held GPS with elevations checked against 1:25000 maps. Skyline measurements were taken using a compass-clinometer at all sites with the topographic shielding factors calculated using the skyline calculator within the CRONUS online calculator (Balco et al., 2008; [http://hess.ess.washington.edu/math/general/skyline\\_input.php](http://hess.ess.washington.edu/math/general/skyline_input.php); accessed on 14<sup>th</sup> September 2015). Sample information is shown in Table 2. Sample photos are shown in Figures 5 (Glen Brittle) and 6 (Soay).

### *3.2.2 Processing*

The thickness and dry bulk density of samples from each site was measured before samples for  $^{36}\text{Cl}$  analysis were crushed and sieved to 250-500  $\mu\text{m}$  at the University of St Andrews. About 2 g of material was retained for elemental analysis with the remainder sent to University of New Hampshire for further preparation and isotopic extraction. Chlorine was extracted and purified from whole-rock samples to produce AgCl for accelerator mass spectrometry (AMS) analysis, following a modified version of procedures developed by Stone et al. (1996). Crushed samples were sonicated first in distilled water and then in 2%  $\text{HNO}_3$  to remove any secondary material attached to grains. 13-20 g of pretreated rock was prepared from each sample for subsequent chemical procedures. Samples were spiked with  $\sim 0.48$  g of isotopically enriched carrier ( $^{35}\text{Cl}/^{37}\text{Cl} = 999 \pm 4$ , total Cl concentration =  $3.65 \text{ mg g}^{-1}$ ) before dissolution in an HF –

HNO<sub>3</sub> solution. Following complete dissolution, aqueous samples were separated from solid fluoride residue by centrifuging, and ~1 ml of 5% AgNO<sub>3</sub> solution was added to precipitate AgCl (and Ag<sub>2</sub>SO<sub>4</sub> if sulfates were present). The precipitate was collected by centrifuging and dissolved in NH<sub>4</sub>OH solution. To remove sulfates, ~1 ml of saturated (BaNO<sub>3</sub>)<sub>2</sub> was added to precipitate BaSO<sub>4</sub>. Final precipitation of AgCl from the aqueous solution was accomplished by addition of 2 M HNO<sub>3</sub> and 5% AgNO<sub>3</sub>. The final AgCl precipitate was collected by centrifuging, washed repeatedly with 18.2 MΩ-cm deionized water, and dried. Approximately 1.5 – 1.75 mg of purified AgCl target material was produced from each sample for AMS measurement.

### 3.2.2 Analysis and age calculations

<sup>36</sup>Cl measurements were carried out at the 5 MV French accelerator mass spectrometry national facility ASTER at CEREGE (Arnold et al., 2013). Use of an isotopically enriched carrier allows simultaneous measurement of <sup>35</sup>Cl/<sup>37</sup>Cl and determination of the natural Cl content of the dissolved samples. For normalization of <sup>36</sup>Cl/<sup>35</sup>Cl ratios, calibration material ‘KN1600’ prepared by K. Nishiizumi, was used. This has a given <sup>36</sup>Cl/<sup>35</sup>Cl value of  $2.11 \pm 0.06 \times 10^{-12}$  (Fifield et al., 1990). Typical uncertainties for raw AMS data are 0.3 – 1.2% for <sup>35</sup>Cl/<sup>37</sup>Cl and 4.8 – 8.0% for <sup>36</sup>Cl/<sup>35</sup>Cl. All samples have <sup>36</sup>Cl/<sup>35</sup>Cl ratios in the range of  $3.8 - 6.9 \times 10^{-14}$  compared to two process blanks (CLBLK7 and 8) with <sup>36</sup>Cl/<sup>35</sup>Cl ratios of  $7.83 \pm 1.0$  and  $4.15 \pm 0.75 \times 10^{-15}$ , respectively. Resulting blank corrections therefore range between 3.4 and 18.1%. Measurement results and calculated concentrations with uncertainties are shown in Table 3.

<sup>36</sup>Cl CRE ages were calculated using the CRONUScalc online calculator

(<http://web1.ittc.ku.edu:8888>; accessed 09/02/2016; Marrero et al., 2016a) and a freely available spreadsheet (Schimmelpfennig et al., 2009).  $^{36}\text{Cl}$  production rates for spallation (Ca, K) have recently been updated by Marrero et al. (2016b). Consequently, we calculated our exposure ages using sea level-high latitude  $^{36}\text{Cl}$  production rates of  $56.0 \pm 4.1$ ,  $155 \pm 11$ ,  $13 \pm 3$  and  $1.9 \pm 0.2$  atoms  $^{36}\text{Cl} \text{ g}^{-1} \text{ a}^{-1}$ , for Ca, K, Ti and Fe, respectively (Marrero et al., 2016b; Schimmelpfennig et al., 2009). In comparison, previous production rates for Ca and K were  $42.2 \pm 4.8$ ,  $145.5 \pm 7.7$  atoms  $^{36}\text{Cl} \text{ g}^{-1} \text{ a}^{-1}$  (Schimmelpfennig et al., 2011, 2014; also see Braucher et al., 2011). We report CRE ages calculated using both Ca and K production rates and scaled for latitude and altitude according to Stone (2000), as adapted by Balco et al. (2008), and Lifton et al. (2014) for comparison. CRE ages were calculated assuming no erosion. Correcting for  $1 \text{ mm ka}^{-1}$  erosion would vary exposure ages by 1-2%. The chemical composition of representative bulk material was determined for each individual sample at the Facility for Earth and Environmental Analysis at the University of St Andrews using X-ray fluorescence (XRF) for major elements and inductively coupled plasma mass spectrometry (ICP-MS) for minor and trace elements. The composition of individual samples is shown in Table 4.

### 3.3 Comparison to proximal marine cores:

We compare our surface exposure dating of the marine terminating Barra-Donnegal Ice Stream with two proximal marine records, MD02-2822 (Hibbert, 2011; Hibbert et al., 2010) and MD01-2461 (Peck et al., 2006, 2008). Giant piston core MD04-2822 was recovered by the RV *Marion Dufresne* from the deep-water margins of the BDF in the Rockall Trough (Figure 1;  $56^{\circ} 50.54' \text{ N}$ ,  $11^{\circ} 22.96' \text{ W}$ ; 2344 m water depth, recovered

in 2004). MD01-2461 was collected from the north-western flank of the Porcupine Seabight approximately 550 km to the southwest (51°45'N, 12°55'W; 1153 m water depth, recovered in 2001). This region lies within the zone of meridional oscillation of the North Atlantic Polar Front during the last glacial (Knutz et al., 2007; Scourse et al., 2009; Hibbert et al., 2010) and as a result is ideally positioned to record both the prevailing hydrographic conditions and the dynamics of the proximal BIIS.

Each core is plotted on their own age model based on tuning to the Greenland  $\delta^{18}\text{O}$  ice core records (using NGRIP on the GICC05 timescale for MD04-2822 and GISP2 for MD01-2461) and calibrated  $^{14}\text{C}$  dates (Figure 10). We have updated the age model for MD04-2822 using: the most recent calibration dataset (IntCal13; Reimer et al., 2013); age uncertainty estimates for each tie-point (a mean squared estimate incorporating uncertainties from both the ice core chronology and tuning procedure) and; a Bayesian deposition model (Bronk Ramsey and Lee, 2013) (Supplementary Table 1).

## **4. Results**

### ***4.1 Multibeam bathymetry***

The multibeam bathymetric survey of Loch Scavaig reveals numerous features – both glaciogenic and post glacial – of interest. The most conspicuous of these is a large arcuate ridge that spans Loch Scavaig and connects with the observed onshore moraine section found on Soay. The ridge is ~4.5 km long and up to 10 m high in places (Figures 7 and 8). A further small extension (~1 km) of this ridge crosses the Sound of Soay to come onshore on the southern margin of the Cuillin. This ridge is interpreted as a terminal moraine, the Scavaig moraine, that clearly delimits the extent of a glacier that flowed from the central rock basin of the Cuillin and into Loch Scavaig.

The submerged glacial land-system preserved in Loch Scavaig is very different,

both in morphology and scale, from that associated with surging tidewater glaciers in Svalbard (Ottesen et al., 2008) with a lack of megascale glacial lineations, crevasse fills and eskers. In addition, the scale and shape of the Scavaig moraine is strikingly different from thrust moraines in Svalbard, which are up to 1 km across with large debris flow lobes on their distal slopes (Ottesen et al., 2008; Kristensen et al., 2009). The Scavaig moraine is a much smaller feature with a well-defined crest, it is generally arcuate in planform, with an asymmetric profile. These features are consistent with a push moraine formed at the margin of the former glacier, indicating that the Scavaig moraine was not formed by a surging glacier but instead marks a readvance of ice from the Cuillin or a still-stand during overall retreat. The Scavaig moraine is traceable across the floor of Loch Scavaig and onto the island of Soay (Figures 4 and 8). The onshore section aligns exactly with the offshore moraine, is composed of material from the Cuillin where the glacier that deposited the Scavaig moraine must have been sourced. It is therefore clearly part of the same feature.

Within the limits of the large moraine is a suite of shorter but conspicuous linear ridges, most prominent in the east of the survey area and immediately inboard of the large moraine (Figure 8). These are up to 2 km long and 5 m high and are interpreted as recessional moraines formed during deglaciation from the outer limit demarked by the Scavaig moraine.

In the east of the survey area, an area of the sea floor is covered with chaotic, hummocky topography (Figure 8). This bears resemblance to features identified as submarine slope failures in bathymetric studies carried out elsewhere in Scotland (Stoker et al., 2010). In addition, the features occur immediately below a conspicuous failure scarp that occurs on Ben Cleat which forms the eastern shore of Loch Scavaig. This feature is interpreted as a post-glacial rock slope failure. Similar terrestrial features



in Scotland have been linked to glacial debuttressing and seismic activity associated with post-glacial isostatic rebound (Ballantyne and Stone, 2013).

#### *4.2 Surface exposure dating using $^{36}\text{Cl}$ .*

The exposure ages calculated following Schimmelpfennig et al. (2009) and Marrero et al., (2016a, b) are shown in Table 5. Due to the differing ways in which each calculator deals with the numerous production pathways of  $^{36}\text{Cl}$  and the varying compositions of our samples the difference in calculated CRE age is not consistent between samples although the ages calculated using the Lm scaling show general agreement between the Schimmelpfennig calculator (Schimmelpfennig et al., 2009) and CRONUScalc (Marrero et al., 2016a). Notably, the choice of scaling is important when using the new CRONUScalc online calculator with CRE ages calculated using the Lm scaling (Stone et al., 2000; Balco et al., 2008) being up to 14% older than when calculated with the SA scaling (Lifton et al., 2014). The cause of this discrepancy is currently enigmatic. The dependency of the CRE ages on choice scaling scheme makes interpretation difficult as there is the danger of selecting CRE ages to fit pre-existing or favoured hypotheses. However, given the range of production rate calibrations included in the CRONUScalc programme, the improved agreement with observed atmospheric cosmic-ray fluxes obtained using the SA scaling scheme and for simplicity, we focus discussion on CRE ages calculated using CRONUScalc and the SA scaling. We present the alternative CRE age calculations for completeness.

The  $^{36}\text{Cl}$  CRE ages range from  $19.4 \pm 1.7$  to  $12.9 \pm 1.2$  ka. The Glen Brittle samples (BRI01-04) yield CRE ages between  $19.4 \pm 1.7$  and  $15.5 \pm 1.7$  ka while the Soay samples (SOAY1-7) yield CRE ages between  $16.4 \pm 1.5$  and  $12.9 \pm 1.2$  ka. A plot of all  $^{36}\text{Cl}$  CRE ages reveals significant overlap in ages from both locations (Figure 9,

Table 5). The 11 samples combined have a reduced Chi-square ( $\chi^2_R$ ) = 4.51 indicating that they are not a single population and are influenced by geological uncertainty. Given this, and the absence of direct geomorphological correlation between the sampled moraines in Glen Brittle and Soay we consider each sample site individually. The Glen Brittle samples have  $\chi^2_R$  = 1.59 which is an acceptable value for a population with three degrees of freedom (Bevington and Robinson, 2003).

The Soay samples have  $\chi^2_R$  = 2.06 indicating the CRE ages are not a single population. Figure 9 shows two CRE age clusters at ~13 ka and ~15 ka ( $\chi^2_R$  = 0.02 and 0.05, respectively). There are two potential interpretations of these CRE ages. The first is that the younger CRE age population reflects the age of deposition of the Scavaig moraine and that the older CRE ages reflect nuclide inheritance from a previous exposure. An alternative interpretation is that the older CRE ages are representative of the true moraine age and the young CRE ages are the result of some post-depositional adjustment and/or exhumation.

## **5. Discussion**

### *5.2 Time of moraine deposition*

A compilation of exposure ages from boulders suggests that they are more likely to underestimate the true CRE age (Heyman et al., 2011). However, this compilation was solely comprised of  $^{10}\text{Be}$  CRE ages. The greater importance of muons in  $^{36}\text{Cl}$  production (e.g. Stone et al., 1998; Braucher et al., 2013) means  $^{36}\text{Cl}$  CRE ages have a greater propensity for inheritance and thus overestimation of ages. Similarly the more complicated evolution of production rate with depth (cf. Gosses and Philips, 2001) means that erosion and or spalling of boulder surfaces can make CRE ages appear older

than the true boulder age. Despite careful sample selection (Section 3.2.1) the spread in our ages demonstrates that some of our samples were influenced by geological uncertainty. We therefore outline what ages in our view best represent the true moraine age and use these ages as the basis for our interpretation with a general note of caution that our ages may overestimate the true moraine age. We outline some reasons why we consider this less likely however acknowledge it as a possibility.

Given the agreement between the CRE ages from Glen Brittle we consider an arithmetic mean to best represent the timing of moraine deposition. Thus we infer that the Glen Brittle moraines were most likely deposited at  $17.6 \pm 1.3$  ka, the mean of our ages. At this time relative sea level (RSL) around the south coast of Skye was high (Figure 11) and the termination of high shorelines is associated with the dated moraines in Glen Brittle. This led Walker et al. (1988) to speculate that at the time of high RSL ice occupied Glen Brittle, a view supported by our CRE ages. We note that there is considerable spread in the ages from Glen Brittle and that the mean age may over- or underestimate the true moraine age.

As stated in section 4.2 there are two possible interpretations of the exposure ages from Soay. We consider it unlikely that nuclide inheritance would affect the other boulders to the same degree such that they yielded internally consistent CRE ages that give an acceptable  $\chi^2_R$  value. Additionally, the young CRE ages suggest moraine deposition prior to the LLR ( $\approx$  Younger Dryas - 12.9–11.7 ka b2k; Lowe et al., 2008). This would imply ice survival throughout the warm Bølling-Allerød interstadial, a scenario that is considered unlikely in Scotland (Ballantyne and Stone, 2012). If the older CRE age cluster is to be inferred as best representing the true moraine age it does however raise the question of how the three other boulders were exhumed at the same time. We note that these three boulders are located in very close proximity (Figure 4)

and that in comparison to the other sampled boulders they are relatively low lying. Boulder height has been shown to influence the clustering of CRE ages with taller boulders being favoured over shorter boulders (Heyman et al., 2016). Thus while we cannot speculate on the specific mechanism of exhumation the boulder-height relationship identified by Heyman et al. (2016) and the close spatial proximity of the three young Soay samples suggests that contemporaneous exhumation is possible. Given all of these considerations, we favour the second scenario and infer that the Scavaig moraine was most likely deposited  $15.2 \pm 0.9$  ka ago.

The mean ages from the moraines do not agree within their analytical uncertainties which, given the proximity of the sample locations, suggests that they may represent separate glacial events. However, we note that there is considerable overlap between the ages from Glen Brittle and Soay thus we cannot definitively make this conclusion. We therefore propose, as a hypothesis, that two separate readvances occurred on the southern margin of the SID during deglaciation. This hypothesis requires further testing with geochronological data.

### *5.1 Implications for local ice dynamics*

Evidence for readvance of locally nourished ice on Skye has been documented from several localities on the low ground that surrounds the Cuillin (Benn, 1997). Glacio-tectonised sediments, patterns of erratic dispersal and changes in the marine limit, all suggest that locally nourished ice remained dynamically active after its separation from mainland ice. Benn (1997) delimited potential readvance limits of the SID, but whether these were contemporaneous has, thus far, remained untested.

It has previously been suggested that readvance of the SID may have resulted from

the removal of constraints imposed by confluent ice allowing the ice to drain radially away from the high ground (Benn, 1997). To the north of the SID a readvance/stillstand is inferred from ice-thrust subaqueous outwash at Suisnish in southern Raasay (Benn, 1997). This site is likely to have been proximal to an ice margin when the Strollamus moraine was deposited at  $15.9 \pm 1.0$  ka (Small et al., 2012). This similarity in age to the older CRE exposure ages from Soay suggests that readvance of the northern and southern sectors of the SID may have been synchronous within dating uncertainties. Additionally, the CRE ages of the Scavaig moraine from Soay and the  $^{10}\text{Be}$  CRE ages from the Strollamus moraine are the same as a suite of  $^{10}\text{Be}$  CRE ages from moraines delimiting the Wester Ross Readvance (Figure 2), ~60 km to the northwest (Robinson and Ballantyne, 1979; Bradwell et al., 2008b, Ballantyne et al., 2009). While the Strollamus moraine has been interpreted as a medial moraine and thus does not record a readvance, it does indicate the existence of a significant ice mass at the time of the WRR. If the Scavaig moraine represents a later readvance, or our CRE ages overestimate the age the Glen Brittle moraine, then, in combination with the evidence for readvance at Suisnish, it is possible that the Wester Ross Readvance may have been more widespread than previously recognized, and involved readvance of local ice on Skye. If this is the case then it implies a common, and likely climatic trigger such as an increase in precipitation associated with climatic warming (c.f. Ballantyne and Stone, 2012). We note however that the uncertainties associated with our ages prevent definitive correlation of the Scavaig moraine to moraines dated elsewhere in Scotland.

## *5.2 Deglaciation of the BDIS*

The deposition age of the Glen Brittle moraine provides a constraint on final deglaciation of the BDIS as its morphology and lithology demonstrates deposition by

valley glaciers fed from the locally nourished SID. As such, it would not be possible to form moraines in Glen Brittle until BDIS deglaciation was complete. Taken at face value, the  $^{36}\text{Cl}$  CRE ages from Glen Brittle presented here suggest deglaciation of the northern sector of the BDIS had occurred by  $17.6 \pm 1.3$  ka (SA scaling). Use of the Lm scaling makes deglaciation considerably earlier ( $19.9 \pm 1.1$  ka) although the ages do overlap at  $1\sigma$ . Considered alongside existing geochronological control from the north coast of Ireland and Jura (McCabe and Clark, 2003; Clark et al., 2009; Ballantyne et al., 2014) (Figure 1), our data suggest that the entire marine portion of the former BDIS was deglaciated by  $17.6 \pm 1.3$  ka. Notably, this timing of deglaciation compares well to a reduction in delivery of IRD to the adjacent deep-sea core MD04-2822 (Hibbert et al., 2010) (Figure 10G). Previous reconstructions of the BIIS (Clark et al., 2012; Hughes et al., 2016) depict ice persisting on the mid-inner shelf until  $\sim 17$  ka with ice reaching the coastline at 16 ka. Our data from Glen Brittle suggest that deglaciation occurred earlier and that ice may have reached the coastline several ka earlier than previously inferred. Notably use of the Lm scaling to calculate the CRE age would exacerbate this difference.

Numerous oceanic forcing mechanisms have been linked to observations of marine deglaciation within the palaeoenvironment. Eustatically forced changes in sea-level (ESL) rise has been cited as a potentially important factor in deglaciation of other palaeo-ice streams that drained the BIIS (Scourse and Furze, 2001; Haapaniemi et al., 2010; Chiverrell et al., 2013) and an initial eustatic sea level rise occurs at 19 ka (e.g., DeDeckker and Yokoyama, 2009; Lambeck et al., 2014), prior to BDIS deglaciation at  $17.6 \pm 1.3$  ka, as constrained by our data (Figure B).

Additionally, it has been shown that tidal mechanical forcing can impact on grounded ice streams (Murray et al., 2007; Arbic et al., 2008; Rosier et al., 2015). The

469 palaeotidal regime influencing the western ice streams draining the BIIS was enhanced  
470 compared to the present day because the open glacial North Atlantic was characterized  
471 by megatidal amplitudes (tidal ranges > 10 m) in many sectors south of the Iceland-  
472 Faroe-Scotland ridge (Uehara et al., 2006; Scourse et al., submitted). Hitherto it has been  
473 difficult to disentangle the relative influence of tidal amplitudes *vis-à-vis* relative sea  
474 level (RSL) changes but recent modelling efforts have addressed this issue for the BIIS  
475 (Scourse et al., submitted) and generated simulations of the potential influence of  
476 palaeotides on the BDIS (Figure 11). These show an enhanced tidal regime in the period  
477 immediately prior to deglaciation as constrained by the CRE ages from Glen Brittle in  
478 the inner BDIS sector (Figure 11). This raises the possibility that this mechanism is a  
479 potentially important driver of deglaciation. However, these large tidal amplitudes are  
480 associated, in this area, with falling RSL driven by rapid glacio-isostatic uplift which  
481 will have mitigated the impact of large tidal range on, for instance, calving rates and ice  
482 stream velocities. Similarly, the deposition of the Scavaig moraine occurred during a  
483 period of enhanced palaeotidal amplitude but falling RSL (Figure 11). The continuity of  
484 these RSL and palaeotidal trends throughout deglaciation imply that other factors; e.g.  
485 climate, topography, ice sheet internal dynamics; were controlling the higher frequency  
486 BDIS advance/readvance phases documented by the new data.

487 Finally, changes in ocean circulation that allow warmer water to access the calving  
488 front (e.g. Holland et al., 2008) have been cited as a major factor in past deglaciations  
489 (Marcott et al., 2011, Rinterknecht et al., 2014). Records of Nps% and  $\delta^{18}\text{O}_{\text{Nps}}$  in MD04-  
490 2822 and a Mg/Ca sea surface temperature estimate from MD01-2461 (Peck et al.,  
491 2008) (Figure 10C, D, E) show a consistent trend indicating northerly migration of the  
492 polar front during Greenland Interstadial 2 (GI-2). Scourse et al. (2009) cite this oceanic  
493 warming as a driver of a major phase of BIIS deglaciation represented by high IRD

fluxes to the deep sea record from ~23 ka. That the BDIS was likely involved in this is indicated by the IRD records from the proximal cores MD95-2006 (Knutz et al., 2001) and MD04-2822 (Hibbert et al., 2010). The rate at which the BDIS deglaciated in response to GI-2 remains unclear. The IRD record from MD04-2822 retains high IRD fluxes 22-18 ka (Hibbert et al., 2010) indicating that the BIIS, and most likely the BDIS, retained calving margins throughout this period. This implies deglaciation may have been a continuous process with punctuated retreat across the shelf although additional geochronological data from the mid-outer shelf is needed to provide further constraints on the nature of BDIS deglaciation in response to GI-2.

## 6. Conclusions

The data presented here provide insights into the timing of deglaciation of a major palaeo-ice stream that drained a large portion of the former BIIS as well as indicating post-ice stream dynamics of the remnant ice mass. Following de-coupling of ice sourced from mainland Scotland and ice sourced in Skye, our data lead us to hypothesise that there were possibly two local readvances/stillstands at ~17.6 and ~15.2 ka demarked by moraines in Glen Brittle and Loch Scavaig, respectively. Evidence for local readvance of ice sourced in Skye occurs around the periphery of Cuillin and our data suggests that the latter readvance, north and south of the Cuillin, was contemporaneous with the Wester Ross Readvance recorded elsewhere in northern Scotland, strengthening the conclusion that it was climatically forced.

The  $^{36}\text{Cl}$  CRE ages from Glen Brittle provide constraints on the timing of final deglaciation of a major ice stream that drained the former BIIS. They indicate that deglaciation of the BDIS was complete by  $17.6 \pm 1.3$  ka, in general agreement with offshore IRD evidence. The complex production pathways associated with *in situ*-



produced  $^{36}\text{Cl}$  lead to large inherent uncertainties on our data that prevent us from definitively linking deglaciation of the BDIS and subsequent readvance to any one forcing factor. Ultimately, disentangling the relative contribution of the various forcing factors requires further data constraining ice margin retreat on the shelf combined with new and more precise geochronological data that constrains final deglaciation.

## **Acknowledgements**

We thank Joe Licciardi for laboratory access at the University of New Hampshire, USA and preparation of  $^{36}\text{Cl}$  targets. The French national AMS facility ASTER (CEREGE, Aix en Provence) is supported by the INSU/CNRS, the ANR through the "Projets thématiques d'excellence" program for the "Equipements d'excellence" ASTER-CEREGE action, IRD and CEA. We would like to thank Shasta Marrero for helpful and informative discussion on the CRONUScalc online calculator. DS was supported by a SAGES studentship and fieldwork by funds from the QRA and BSG. Detailed comments from two anonymous reviewers have improved the quality and clarity of this manuscript.

535   **References**

- 536   Alley, R.B. and MacAyeal, D.R., 1994. Ice-rafted debris associated with binge/purge  
537       oscillations of the Laurentide Ice Sheet. *Paleoceanography*, 9, 503-511.
- 538   Arbic, B.K., Mitrovica, J.X., MacAyeal, D.R. and Milne, G.A., 2008. On the factors  
539       behind large Labrador Sea tides during the last glacial cycle and the potential  
540       implications for Heinrich events. *Paleoceanography*, 23, PA3211.
- 541   Austin, W.E.N. and Kroon, D., 1996. Late glacial sedimentology, foraminifera and  
542       stable isotope stratigraphy of the Hebridean Continental Shelf, northwest  
543       Scotland. *Geological Society, London, Special Publications*, 111, 187-213.
- 544   Arnold, M., Aumaître, G., Bourlès, D.L., Keddadouche, K., Braucher, R., Finkel, R.C.,  
545       Nottoli, E., Benedetti, L. and Merchel, S., 2013. The French accelerator mass  
546       spectrometry facility ASTER after 4years: Status and recent developments on  
547       <sup>36</sup>Cl and <sup>129</sup>I. *Nuclear Instruments and Methods in Physics Research Section B:*  
548       *Beam Interactions with Materials and Atoms*, 294, 24-28.
- 549   Ballantyne, C.K., 1989, The Loch Lomond Readvance on the Isle of Skye, Scotland:  
550       glacier reconstruction and palaeoclimatic implications: *Journal of Quaternary*  
551       *Science*, 4, 95-108.
- 552   Ballantyne, C.K., and Stone, J.O., 2012, Did large ice caps persist on low ground in  
553       north-west Scotland during the Lateglacial Interstade?: *Journal of Quaternary*  
554       *Science*, 27, 297-306.
- 555   Ballantyne, C.K. and Stone, J.O., 2013. Timing and periodicity of paraglacial rock-slope  
556       failures in the Scottish Highlands. *Geomorphology*, 186, 150-161.
- 557   Ballantyne C.K., Benn, D.I., Lowe, J.J., Walker, M.J.C., (Eds.), 1991, The Quaternary  
558       of the Isle of Skye: Field Guide, Quaternary Research Association, Cambridge.

559 Ballantyne, C.K., Schnabel, C. and Xu, S., 2009. Readvance of the last British–Irish ice  
560 sheet during Greenland interstade 1 (GI-1): the Wester Ross readvance, NW  
561 Scotland. *Quaternary Science Reviews*, 28, 783-789.

562 Ballantyne, C.K., Wilson, P., Gheorghiu, D., and Rodés, À., 2014, Enhanced rock- slope  
563 failure following ice-sheet deglaciation: timing and causes: *Earth Surface  
564 Processes and Landforms*, 39, 900-913.

565 Benn, D.I., 1997. Glacier fluctuations in western Scotland. *Quaternary International*,  
566 38, 137-147.

567 Bennett, M.R., 2003. Ice streams as the arteries of an ice sheet: their mechanics, stability  
568 and significance. *Earth-Science Reviews*, 61, 309-339.

569 Bennett, M.R. and Boulton, G.S., 1993. Deglaciation of the Younger Dryas or Loch  
570 Lomond Stadial ice-field in the northern Highlands, Scotland. *Journal of  
571 Quaternary Science*, 8, 133-145.

572 Baltzer, A., Bates, R., Mokeddem, Z., Clet-Pellerin, M., Walter-Simonnet, A.V.,  
573 Bonnot-Courtois, C. and Austin, W.E., 2010. Using seismic facies and pollen  
574 analyses to evaluate climatically driven change in a Scottish sea loch (fjord) over  
575 the last 20 ka. *Geological Society, London, Special Publications*, 344, 355-369.

576 Berger, A., and Loutre, M.F., 1991, Insolation values for the climate of the last 10  
577 million years. *Quaternary Science Reviews*, 10, 297-317.

578 Bevington, PR and Robinson, D.K., 2003, Data reduction and error analysis: McGraw–  
579 Hill, New York, p. 320.

580 Bradwell, T. and Stoker, M.S., 2015. Submarine sediment and landform record of a  
581 palaeo-ice stream within the British– Irish Ice Sheet. *Boreas*, 44, 255-276.

582 Bradwell, T., Stoker, M.S., Golledge, N.R., Wilson, C.K., Merritt, J.W., Long, D.,  
583 Everest, J.D., Hestvik, O.B., Stevenson, A.G., Hubbard, A.L. and Finlayson,  
584 A.G., 2008a. The northern sector of the last British Ice Sheet: maximum extent  
585 and demise. *Earth-Science Reviews*, 88, 207-226.

586 Bradwell, T., Fabel, D., Stoker, M., Mathers, H., McHargue, L. and Howe, J., 2008b. Ice  
587 caps existed throughout the Lateglacial Interstadial in northern Scotland. *Journal*  
588 *of Quaternary Science*, 23, 401-407.

589 Braucher, R., Merchel, S., Borgomano, J. and Bourlès, D.L., 2011. Production of  
590 cosmogenic radionuclides at great depth: A multi element approach. *Earth and*  
591 *Planetary Science Letters*, 309, 1-9.

592 Bronk Ramsey, C., 2008. Deposition models for chronological records. *Quaternary*  
593 *Science Reviews*, 27, 42-60.

594 Bronk Ramsey, C., 2013. OxCal 4.2. *Manual [online] available at: [https://c14.arch.ox.](https://c14.arch.ox.ac.uk/oxcalhelp/hlp_contents.html)*  
595 *ac.uk/oxcalhelp/hlp\_contents.html*.

596 Bronk Ramsey, C. and Lee, S., 2013. Recent and planned developments of the program  
597 OxCal. *Radiocarbon*, 55, 720-730.

598 Clark, C.D., Evans, D.J., Khatwa, A., Bradwell, T., Jordan, C.J., Marsh, S.H., Mitchell,  
599 W.A. and Bateman, M.D., 2004. Map and GIS database of glacial landforms and  
600 features related to the last British Ice Sheet. *Boreas*, 33, 359-375.

601 Clark, C.D., Hughes, A.L., Greenwood, S.L., Jordan, C., and Sejrup, H.P., 2012, Pattern  
602 and timing of retreat of the last British-Irish Ice Sheet: *Quaternary Science*  
603 *Reviews*, 44, 112-146.

604 Clark, J., McCabe, A.M., Schnabel, C., Clark, P.U., McCarron, S., Freeman, S.P.,  
605 Maden, C. and Xu, S., 2009. Cosmogenic <sup>10</sup>Be chronology of the last

606            deglaciation of western Ireland, and implications for sensitivity of the Irish Ice  
 607            Sheet to climate change. *Geological Society of America Bulletin*, 121, 3-16.  
 608    Clough, C.T. and Harker, A., 1904. *The Geology of West-Central Skye, with Soay:*  
 609            *Explanation of* (Vol. 70). HM Stationery Office.  
 610    Chiverrell, R.C., Thrasher, I.M., Thomas, G.S., Lang, A., Scourse, J.D., van  
 611            Landeghem, K.J., Mccarroll, D., Clark, C.D., Cofaigh, C.Ó., Evans, D.J. and  
 612            Ballantyne, C.K., 2013. Bayesian modelling the retreat of the Irish Sea Ice  
 613            Stream. *Journal of Quaternary Science*, 28(2), pp.200-209.  
 614    De Deckker, P. and Yokoyama, Y., 2009. Micropalaeontological evidence for Late  
 615            Quaternary sea-level changes in Bonaparte Gulf, Australia. *Global and*  
 616            *Planetary Change*, 66, 85-92.  
 617    Deschamps, P., Durand, N., Bard, E., Hamelin, B., Camoin, G., Thomas, A.L.,  
 618            Henderson, G.M., Okuno, J.I. and Yokoyama, Y., 2012. Ice-sheet collapse and  
 619            sea-level rise at the Bolling warming 14,600 years ago. *Nature*, 483, 559-564.  
 620    Dove, D., Arosio, R., Finlayson, A., Bradwell, T. and Howe, J.A., 2015. Submarine  
 621            glacial landforms record Late Pleistocene ice-sheet dynamics, Inner Hebrides,  
 622            Scotland. *Quaternary Science Reviews*, 123, 76-90.  
 623    Dowdeswell, J.A., Hogan, K.A., Cofaigh, C.Ó., Fugelli, E.M.G., Evans, J. and  
 624            Noormets, R., 2014. Late Quaternary ice flow in a West Greenland fjord and  
 625            cross-shelf trough system: submarine landforms from Rink Isbrae to  
 626            Uummannaq shelf and slope. *Quaternary Science Reviews*, 92, 292-309.  
 627    Dunlop, P., Shannon, R., McCabe, M., Quinn, R., and Doyle, E., 2010, Marine  
 628            geophysical evidence for ice sheet extension and recession on the Malin Shelf:  
 629            New evidence for the western limits of the British Irish Ice Sheet: *Marine*  
 630            *Geology*, 276, 86-99.

631 Fabel, D., Ballantyne, C.K. and Xu, S., 2012. Trimlines, blockfields, mountain-top  
632 erratics and the vertical dimensions of the last British–Irish Ice Sheet in NW  
633 Scotland. *Quaternary Science Reviews*, 55, 91-102.

634 Fifield, L.K., Ophel, T.R., Allan, G.L., Bird, J.R. and Davie, R.F., 1990. Accelerator  
635 mass spectrometry at the Australian National University's 14UD accelerator:  
636 experience and developments. *Nuclear Instruments and Methods in Physics  
637 Research Section B: Beam Interactions with Materials and Atoms*, 52, 233-237.

638 Haapanieni, A.I., Scourse, J.D., Peck, V.L., Kennedy, D.P., Kennedy, H., Hemming,  
639 S.R., Furze, M.F.A., Pieńkowski-Furze, A.J., Walden, J., Wadsworth, E. and  
640 Hall, I.R. 2010. Source, timing, frequency and flux of ice-rafted detritus to the  
641 Northeast Atlantic margin, 30-12 ka: testing the Heinrich precursor hypothesis.  
642 *Boreas*, 39, 576-591.

643 Harker, A., 1901. Ice-erosion in the Cuillin Hills, Skye: *Transactions of the Royal  
644 Society of Edinburgh*, 40, 221–252.

645 Heyman, J., Stroeve, A.P., Harbor, J.M., and Caffee, M.W., 2011, Too young or too  
646 old: evaluating cosmogenic exposure dating based on an analysis of compiled  
647 boulder exposure ages: *Earth and Planetary Science Letters*, 302, 71-80.

648 Hibbert FD. 2011. Dynamics of the British Ice Sheet and Prevailing Hydrographic  
649 Conditions for the Last 175,000 years: An investigation of marine sediment core  
650 MD04-2822 from the Rockall Trough. *Unpublished PhD thesis, University of St  
651 Andrews*.

652 Hibbert, F.D., Austin, W.E., Leng, M.J., and Gatliff, R.W., 2010, British Ice Sheet  
653 dynamics inferred from North Atlantic ice-rafted debris records spanning the last  
654 175 000 years: *Journal of Quaternary Science*, 25, 461-482.

655 Holland, D.M., Thomas, R.H., De Young, B., Ribergaard, M.H., and Lyberth, B., 2008,  
 656 Acceleration of Jakobshavn Isbrae triggered by warm subsurface ocean waters:  
 657 *Nature Geoscience*, 1, 659-664.

658 Howe, J.A., Dove, D., Bradwell, T. and Gafeira, J., 2012. Submarine geomorphology  
 659 and glacial history of the Sea of the Hebrides, UK. *Marine Geology*, 315, 64-76.

660 Hubbard, A., Bradwell, T., Golledge, N., Hall, A., Patton, H., Sugden, D., Cooper, R.  
 661 and Stoker, M., 2009. Dynamic cycles, ice streams and their impact on the  
 662 extent, chronology and deglaciation of the British–Irish ice sheet. *Quaternary*  
 663 *Science Reviews*, 28, 758-776.

664 Joughin, I., Smith, B.E., and Medley, B., 2014, Marine ice sheet collapse potentially  
 665 under way for the Thwaites Glacier Basin, West Antarctica: *Science*, 344, 735-  
 666 738.

667 Knutz, P.C., Austin, W.E., and Jones, E.J.W., 2001, Millennial- scale depositional cycles  
 668 related to British Ice Sheet variability and North Atlantic paleocirculation since  
 669 45 kyr BP, Barra Fan, UK margin: *Paleoceanography*, 16, 53-64.

670 Knutz, P.C., Zahn, R., and Hall, I.R., 2007, Centennial- scale variability of the British  
 671 Ice Sheet: Implications for climate forcing and Atlantic meridional overturning  
 672 circulation during the last deglaciation: *Paleoceanography* 22.

673 Kristensen, L., Benn, D.I., Holmes, A. and Ottesen, D. 2009. Mud aprons in front of  
 674 Svalbard surge moraines: evidence of subglacial deforming layers or proglacial  
 675 tectonics? *Geomorphology* 111, 206-221.

676 Lambeck, K., Rouby, H., Purcell, A., Sun, Y., and Sambridge, M., 2014, Sea level and  
 677 global ice volumes from the Last Glacial Maximum to the Holocene:

678           *Proceedings of the National Academy of Science of the United States of America*,  
679           111, 15296-15303.

680   Lifton, N., Sato, T. and Dunai, T.J., 2014. Scaling in situ cosmogenic nuclide production  
681           rates using analytical approximations to atmospheric cosmic-ray fluxes. *Earth*  
682           *and Planetary Science Letters*, 386, pp.149-160.

683   Livingstone, S.J., Cofaigh, C.Ó., Stokes, C.R., Hillenbrand, C.D., Vieli, A. and  
684           Jamieson, S.S., 2013. Glacial geomorphology of Marguerite Bay palaeo-ice  
685           stream, western Antarctic Peninsula. *Journal of Maps*, 9, 558-572.

686   Lowe, J.J., Rasmussen, S.O., Björck, S., Hoek, W.Z., Steffensen, J.P., Walker, M.J. and  
687           Yu, Z.C., 2008. Synchronisation of palaeoenvironmental events in the North  
688           Atlantic region during the Last Termination: a revised protocol recommended by  
689           the INTIMATE group. *Quaternary Science Reviews*, 27, 6-17.

690   Marcott, S.A., Clark, P.U., Padman, L., Klinkhammer, G.P., Springer, S.R., Liu, Z.,  
691           Otto-Bliesner, B.L., Carlson, A.E., Ungerer, A., Padman, J. and He, F., 2011.  
692           Ice-shelf collapse from subsurface warming as a trigger for Heinrich events.  
693           *Proceedings of the National Academy of Sciences*, 108, 13415-13419.

694   Marrero, S.M., Phillips, F.M., Borchers, B., Lifton, N., Aumer, R. and Balco, G., 2016a.  
695           Cosmogenic nuclide systematics and the CRONUScale program. *Quaternary*  
696           *Geochronology*, 31, 160-187.

697   Marrero, S.M., Phillips, F.M., Caffee, M.W. and Gosse, J.C., 2016b. CRONUS-Earth  
698           cosmogenic <sup>36</sup>Cl calibration. *Quaternary Geochronology*, 31, 199-219.

699   McCabe, A.M., and Clark, P.U., 2003, Deglacial chronology from County Donegal,  
700           Ireland: implications for deglaciation of the British–Irish ice sheet: *Journal of the*  
701           *Geological Society of London*, 160, 847-855.



702 Murray, T., Smith, A.M., King, M.A. and Weedon, G.P., 2007. Ice flow modulated by  
703 tides at up to annual periods at Rutford Ice Stream, West Antarctica. *Geophysical*  
704 *Research Letters*, 34, L18503.

705 Ó' Cofaigh, C., Dunlop, P. and Benetti, S., 2012. Marine geophysical evidence for Late  
706 Pleistocene ice sheet extent and recession off northwest Ireland. *Quaternary*  
707 *Science Reviews*, 44, 147-159.

708 Ottesen, D., Dowdeswell, J.A., Benn, D.I., Kristensen, L., Christiansen, H.H.,  
709 Christensen, O., Hansen, L., Lebesbye, E., Forwick, M. and Vorren, T.O., 2008.  
710 Submarine landforms characteristic of glacier surges in two Spitsbergen fjords.  
711 *Quaternary Science Reviews*, 27, 1583-1599.

712 Peacock, J.D., 2008, Late Devensian palaeoenvironmental changes in the sea area  
713 adjacent to Islay, SW Scotland: implications for the deglacial history of the  
714 island: *Scottish Journal of Geology*, 44, 183-190.

715 Peacock, J.D., Austin, W.E.N., Selby, I., Graham, D.K., Harland, R. and Wilkinson, I.P.,  
716 1992. Late Devensian and Flandrian palaeoenvironmental changes on the  
717 Scottish continental shelf west of the Outer Hebrides. *Journal of Quaternary*  
718 *Science*, 7, 145-161.

719 Peck, V.L., Hall, I.R., Zahn, R., and Elderfield, H., 2008, Millennial-scale surface and  
720 subsurface paleothermometry from the northeast Atlantic, 55–8 ka BP:  
721 *Paleoceanography*, 23, PA3221.

722 Peck, V.L., Hall, I.R., Zahn, R., Grousset, F., Hemming, S.R. and Scourse, J.D., 2007.  
723 The relationship of Heinrich events and their European precursors over the past  
724 60ka BP: a multi-proxy ice-rafted debris provenance study in the North East  
725 Atlantic. *Quaternary Science Reviews*, 26(7), 862-875.

726 Rasmussen, S.O., Seierstad, I.K., Andersen, K.K., Bigler, M., Dahl-Jensen, D., and  
 727 Johnsen, S.J., 2008, Synchronization of the NGRIP, GRIP, and GISP2 ice cores  
 728 across MIS 2 and palaeoclimatic implications: *Quaternary Science Reviews*, 27,  
 729 18-28.

730 Rinterknecht, V., Jomelli, V., Brunstein, D., Favier, V., Masson-Delmotte, V., Bourlès,  
 731 D., Leanni, L. and Schläppy, R., 2014. Unstable ice stream in Greenland during  
 732 the Younger Dryas cold event. *Geology*, 42, 759-762.

733 Robinson, M. and Ballantyne, C.K., 1979. Evidence for a glacial readvance pre-dating  
 734 the Loch Lomond Advance in Wester Ross. *Scottish Journal of Geology*, 15,  
 735 271-277.

736 Rosier, S.H.R., Gudmundsson, G.H. and Green, J.A.M. 2015. Temporal variations in  
 737 the flow of a large Antarctic ice-stream controlled by tidally induced changes in  
 738 the subglacial water system. *Cryosphere*, 9, 2397-2429.

739 Schimmelpfennig, I., Benedetti, L., Finkel, R., Pik, R., Blard, P. H., Bourlès, D.,  
 740 Burnard, P., and Williams, A., 2009, Sources of in-situ  $^{36}\text{Cl}$  in basaltic rocks.  
 741 Implications for calibration of production rates: *Quaternary Geochronology*, 4,  
 742 441-461.

743 Schimmelpfennig, I., Benedetti, L., Garreta, V., Pik, R., Blard, P.H., Burnard, P.,  
 744 Bourlès, D., Finkel, R., Ammon, K., and Dunai, T., 2011, Calibration of  
 745 cosmogenic  $^{36}\text{Cl}$  production rates from Ca and K spallation in lava flows from  
 746 Mt. Etna (38° N, Italy) and Payun Matru (36° S, Argentina): *Geochimica et*  
 747 *Cosmochimic Acta*, 75, 2611-2632.

748 Schimmelpfennig, I., Schaefer, J.M., Putnam, A.E., Koffman, T., Benedetti, L.,  
 749 Ivy-Ochs, S., ASTER team, and Schlüchter, C., 2014,  $^{36}\text{Cl}$  production rate from

750 K-spallation in the European Alps (Chironico landslide, Switzerland): *Journal of*  
751 *Quaternary Science*, 29, 407-413.

752 Scourse, J.D. and Furze, M.F.A., 2001. A critical review of the glaciomarine model for  
753 Irish Sea deglaciation: evidence from southern Britain, the Celtic shelf and  
754 adjacent continental slope. *Journal of Quaternary Science*, 16, 419-434.

755 Scourse, J.D., Hall, I.R., McCave, I.N., Young, J.R. and Sugdon, C., 2000. The origin of  
756 Heinrich layers: evidence from H2 for European precursor events. *Earth and*  
757 *Planetary Science Letters*, 182(2), pp.187-195.

758 Scourse, J.D., Haapaniemi, A.I., Colmenero-Hidalgo, E., Peck, V.L., Hall, I.R., Austin,  
759 W.E., Knutz, P.C. and Zahn, R., 2009. Growth, dynamics and deglaciation of the  
760 last British-Irish ice sheet: the deep-sea ice-rafted detritus record. *Quaternary*  
761 *Science Reviews*, 28(27), 3066-3084.

762 Scourse, J.D., Ward, S.L., Wainwright, A., Bradley, S.L. and Uehara, K. Submitted. The  
763 role of megatides and relative sea level in controlling the deglaciation of the  
764 British-Irish and Fennoscandian Ice Sheets. *Journal of Quaternary Science*.

765 Seierstad, I.K., Abbott, P.M., Bigler, M., Blunier, T., Bourne, A.J., Brook, E., Buchardt,  
766 S.L., Buizert, C., Clausen, H.B., Cook, E. and Dahl-Jensen, D., 2014.  
767 Consistently dated records from the Greenland GRIP, GISP2 and NGRIP ice  
768 cores for the past 104 ka reveal regional millennial-scale  $\delta^{18}\text{O}$  gradients with  
769 possible Heinrich event imprint. *Quaternary Science Reviews*, 106, pp.29-46.

770 Sejrup, H.P., Larsen, E., Landvik, J., King, E.L., Haflidason, H. and Nesje, A., 2000.  
771 Quaternary glaciations in southern Fennoscandia: evidence from southwestern  
772 Norway and the northern North Sea region. *Quaternary Science Reviews*, 19,  
773 667-685.

774    Sissons, J.B., Lowe, J.J., Thompson, K.S. and Walker, M.J.C., 1973. Loch Lomond  
 775            readvance in Grampian Highlands of Scotland: *Nature*, 244, 75-77.

776    Small, D., 2012 The Deglaciation of the northwest sector of the last British-Irish Ice  
 777            Sheet: Integrating onshore and offshore data relating to chronology and  
 778            behaviour. *Unpublished PhD Thesis, University of St Andrews*.

779    Small, D., Rinterknecht, V., Austin, W., Fabel, D. and Miguens-Rodriguez, M., 2012,  
 780            In situ cosmogenic exposure ages from the Isle of Skye, northwest Scotland:  
 781            implications for the timing of deglaciation and readvance from 15 to 11 ka.  
 782            *Journal of Quaternary Science*, 27, 150-158.

783    Small D., Austin W., and Rinterknecht V., 2013. Freshwater influx, hydrographic  
 784            reorganization and the dispersal of ice-rafted detritus in the sub-polar North  
 785            Atlantic Ocean during the last deglaciation: *Journal of Quaternary Science*, 28,  
 786            527-535.

787    Stoker, M. and Bradwell, T., 2005. The Minch palaeo-ice stream, NW sector of the  
 788            British–Irish Ice Sheet. *Journal of the Geological Society*, 162, 425-428.

789    Stoker, M.S., Wilson, C.R., Howe, J.A., Bradwell, T. and Long, D., 2010. Paraglacial  
 790            slope instability in Scottish fjords: examples from Little Loch Broom, NW  
 791            Scotland. *Geological Society, London, Special Publications*, 344, 225-242.

792    Stokes, C.R. and Clark, C.D., 2001. Palaeo-ice streams. *Quaternary Science Reviews*,  
 793            20, 1437-1457.

794    Stokes, C.R., Tarasov, L., Blomdin, R., Cronin, T.M., Fisher, T.G., Gyllencreutz, R.,  
 795            Hättestrand, C., Heyman, J., Hindmarsh, R.C., Hughes, A.L. and Jakobsson, M.,  
 796            2015. On the reconstruction of palaeo-ice sheets: Recent advances and future  
 797            challenges. *Quaternary Science Reviews*, 125, 15-49.

798 Stone, J.O., 2000, Air pressure and cosmogenic isotope production: *Journal of*  
799 *Geophysical Research: Solid Earth*, 105, 23753-23759.

800 Stone, J.O., Allan, G.L., Fifield, L.K. and Cresswell, R.G., 1996. Cosmogenic chlorine-  
801 36 from calcium spallation. *Geochimica et Cosmochimica Acta*, 60, 679-692.

802 Stone, J.O., Ballantyne, C.K. and Fifield, L.K., 1998. Exposure dating and validation of  
803 periglacial weathering limits, northwest Scotland. *Geology*, 26, 587-590.

804 Svendsen, J.I., Briner, J.P., Mangerud, J. and Young, N.E., 2015. Early break-up of the  
805 Norwegian channel ice stream during the last glacial maximum. *Quaternary*  
806 *Science Reviews*, 107, 231-242.

807 Uehara, K., Scourse, J.D., Horsburgh, K.J., Lambeck, K. and Purcell, A.P., 2006. Tidal  
808 evolution of the northwest European shelf seas from the Last Glacial Maximum  
809 to the present. *Journal of Geophysical Research: Oceans*, 111, C09025.

810 Walker, M.J., Ballantyne, C.K., Lowe, J.J. and Sutherland, D.G., 1988. A  
811 reinterpretation of the Lateglacial environmental history of the Isle of Skye,  
812 Inner Hebrides, Scotland. *Journal of Quaternary Science*, 3, 135-146.

813 Wouters, B., Martin-Español, A., Helm, V., Flament, T., van Wessem, J.M., Ligtnerberg,  
814 S.R.M., van den Broeke, M.R., and Bamber, J. L., 2015, Dynamic thinning of  
815 glaciers on the Southern Antarctic Peninsula: *Science*, 348, 899-903.

816

# **Figure Captions**

818 Figure 1. Google Earth Image with extent of the BDIS and related glaciological features.  
819 Existing geochronological dates are shown (Table 1) along with location of marine core  
820 MD04-2822. Flowlines adjusted from Bradwell et al. (2008). Dashed box shows the  
821 location of Figure 2, solid box shows location of Figure 7. Isochrones depicting the most  
822 likely ice extent at 24 ka, 17 ka, and 16 ka (shaded for clarity) are taken from Hughes et

al., 2016. BDF = Barra/Donegal Fan, BDIS = Barra/Donegal Ice Stream, MIS = Minch Ice Stream. All  $^{10}\text{Be}$  CRE dates have been re-calculated using a local production rate (Loch Lomond Production Rate) of  $3.92 \pm 0.18 \text{ atoms g}^{-1} \text{ a}^{-1}$  (Fabel et al., 2012).

Figure 2. Location map of Skye and northwest Scotland showing locations mentioned in text. Dashed lines demark inferred zones of confluence between mainland ice and the Skye Ice Dome. Red stars show locations of existing exposure ages from (1) Trotternish (Stone et al., 1998) and (2) the Strollamus moraine (Small et al., 2012). GB = Glen Brittle, LS = Loch Scavaig. Arrows show generalized ice flow directions, MIS = Minch Ice Stream, BDIS = Barra-Donegal Ice Stream. Also shown are inferred limits of Wester Ross Readvance (WRR). Letters A and B denote the locations of the palaeotidal and RSL simulations (Section 5.2; Figure 11). DEM derived from NASNA SRTM 90 m data, available at <http://www.sharegeo.ac.uk/handle/10672/5>.

Figure 3. Map of Glen Brittle area showing sampled moraines, raised shorelines and locations of sampled boulders. The limits of the Loch Lomond Readvance and associated landforms are shown as adapted from Ballantyne (1989). Contours at 100 m intervals. See Figure 5 for location.

Figure 4. Map of the northeast corner of Soay showing sampled moraine and locations of sampled boulders. Dashed line shows crest of offshore moraine (Figure 8).

Figure 5. Site and sample photographs from Glen Brittle. (A) Glen Brittle looking North. Showing two parallel moraine ridges. Southern (outer) moraine with person, northern

(inner) moraine with boulders on near horizon. Ice flow is towards the camera. (B) BRI01 boulder. (C) BRI-02 boulder. (D) BRI-03 boulder. (E) BRI-04 boulder.

Figure 6. Site and sample photographs from Soay. (A) SOAY1 boulder. (B) SOAY2 boulder. (C) SOAY3 boulder. (D) SOAY4 boulder. (E) SOAY5 boulder. (F) SOAY6 boulder. (G) SOAY7 boulder. (H) Soay moraine onshore. The dashed white line marks the crest. The offshore continuation stretches across Loch Scavaig to the far shore (see Figures 5 and 6). Samples were located off-shot in the wooded area to the right. Ice flow was from left to right.

Figure 7. Location of  $^{36}\text{Cl}$  samples presented and onshore moraines in Glen Brittle and on Soay. The multibeam bathymetry of Loch Scavaig is shown alongside mapped YD ice limits modified from Ballantyne (1989). Note the distinctive offshore moraine that impinges on Soay. Failure scarp and extent of inferred slope failure (SF) is also shown. The red star in the upper right is the location of the dated Strollamus medial moraine (Benn, 1990; Small et al., 2012). NEXTmap hillshade DEM by Intermap Technologies.

Figure 8. Interpreted bathymetric map of Loch Scavaig showing the distinctive arcuate terminal moraine. Suites of recessional moraines are also highlighted. There is a distinctive glacially over-deepened basin in the western portion of the survey area. The trench in the northeastern sector is the offshore continuation of the Camasunary Fault. The red star shows the location of the vibrocore VC57/-07/844 which yielded a basal radiocarbon age of  $12.8 \pm 0.1$  ka (Small, 2012). Also show is the failure scarp on Ben Cleat and the associated landslide deposits. NEXTmap hillshade DEM by Intermap Technologies.

872

873 Figure 9. Summary CRE age plot of  $^{36}\text{Cl}$  samples presented here shown alongside the  
874 NGRIP oxygen isotope record ( $\delta^{18}\text{O}$ , ‰) (Rasmussen et al., 2008). Grey boxes show  
875 arithmetic means and uncertainties of Brittle and Soay samples respectively. The Soay  
876 samples not included in calculating moraine ages shown with hollow circles.  
877 Uncertainties are  $1\sigma$  analytical uncertainties. The Younger Dryas stadial (YD) and  
878 Bølling-Allerød interstadial are also shown (B-A).

879

880 Figure 10. Proxy records of deglacial forcing for the time period of BDIS deglaciation  
881 indicated by the shaded column. (A) Greenland oxygen isotope records ( $\delta^{18}\text{O}$ , ‰) from  
882 NGRIP, GRIP and GISP2 on the GICC05 timescale (Rasmussen et al., 2008; Seierstad  
883 et al., 2014) [50 yr moving averages shown by black line] (B) Reconstructed ESL  
884 (Lambeck et al., 2014). Proxies relating to oceanic forcing: (C) Mg/Ca (*G.bulloides*)  
885 SST estimates from MD01-2461 (Porcupine Seabight, Peck et al., 2008); and MD04-  
886 2822 (Rockall Trough, Hibbert, 2011; Hibbert et al., 2010) (D)  $\delta^{18}\text{O}$  *N.pachyderma*  
887 sinistral (‰ VPDB), (E) % *N.pachyderma* (sinistral), (F) XRF core scanning (ITRAX)  
888 TiCa (proxy for terrigenous input) and, (G) total IRD flux ( $> 150 \mu\text{m cm}^{-2} \text{ka}^{-1}$ ).

889

890 Figure 11. Relative sea level (RSL) and palaeotidal (PTM) simulations for two locations  
891 in the inner part of the BDIS adjacent to Skye. A)  $57.04^\circ \text{N}$ ,  $6.88^\circ \text{W}$  and, B)  $57.12^\circ \text{N}$ ,  
892  $6.13^\circ \text{W}$  (see Figure 2 for locations). RSL simulations are based on the modified glacio-  
893 isostatic adjustment model of Lambeck and PTM simulations on a modified version of  
894 the Princeton Ocean Model forced with dynamic open ocean tide (Uehara et al., 2006).  
895 These show mean *M2* tidal ranges  $> 6 \text{ m}$  throughout the deglacial phase from the Last  
896 Glacial Maximum to around 11 ka BP (spring tidal ranges would have been significantly



897 larger). The shaded boxes in A and B show the mean exposure ages from Glen Brittle  
898 and Soay, respectively.  
899

Table 1. Published ages referred to in the text and shown on Figure 1. Outliers are shown in italics. Clusters of CRE ages that yield acceptable  $\chi_R^2$  values are shown in bold, the mean of these is shown in Figure 1. Underlined radiocarbon ages are the oldest from a site and these are used in Figure 1. CRE ages calculated using CRONUS online calculator (<http://hess.ess.washington.edu>; accessed April 20th 2016), Lm scaling and, Loch Lomond Production Rate of  $3.92 \pm 0.18$  atoms  $\text{g}^{-1} \text{yr}^{-1}$  (Fabel et al. 2012).  $^{14}\text{C}$  ages calibrated using OxCal 4.2 (Bronk Ramsey 2013) and Marine14 (Reimer et al., 2013),  $\Delta R=300$  yr.

Reference	Location (site no. Fig. 1)	Sample name	Technique	Age (yr)	Uncert. (yr)
Clark et al. (2009)	N Donegal coast (1)	BF-04-01	CRE	17607	1772
Clark et al. (2009)	N Donegal coast (1)	BF-04-03	CRE	33035	2940
<b>Clark et al. (2009)</b>	<b>N Donegal coast (1)</b>	<b>BF-04-04</b>	<b>CRE</b>	<b>21463</b>	<b>1754</b>
<b>Clark et al. (2009)</b>	<b>N Donegal coast (1)</b>	<b>BF-04-05</b>	<b>CRE</b>	<b>20924</b>	<b>1863</b>
<b>Clark et al. (2009)</b>	<b>N Donegal coast (1)</b>	<b>BF-04-06</b>	<b>CRE</b>	<b>20949</b>	<b>2060</b>
Clark et al. (2009)	N Donegal coast (1)	BF-04-08	CRE	23251	2135
<b>Clark et al. (2009)</b>	<b>N Donegal coast (1)</b>	<b>BF-04-09</b>	<b>CRE</b>	<b>21428</b>	<b>2196</b>
<b>Clark et al. (2009)</b>	<b>N Donegal coast (1)</b>	<b>BF-04-10</b>	<b>CRE</b>	<b>21799</b>	<b>2190</b>
McCabe & Clark (2003)	N Donegal coast (2)	AA32315	$^{14}\text{C}$	16602	178
McCabe & Clark (2003)	N Donegal coast (2)	AA45968	$^{14}\text{C}$	18676	168
McCabe & Clark (2003)	N Donegal coast (2)	AA45967	$^{14}\text{C}$	17997	188
McCabe & Clark (2003)	N Donegal coast (2)	AA45966	$^{14}\text{C}$	19093	496
McCabe & Clark (2003)	N Donegal coast (2)	AA33831	$^{14}\text{C}$	17913	130
<u>McCabe &amp; Clark (2003)</u>	<u>N Donegal coast (2)</u>	<u>AA33832</u>	<u><math>^{14}\text{C}</math></u>	<u>20308</u>	<u>148</u>
Peacock (2008)	Islay (3)	SUERC-13122	$^{14}\text{C}$	14457	163
Peacock (2008)	Islay (3)	SUERC-13123	$^{14}\text{C}$	14337	149
<u>Peacock (2008)</u>	<u>Islay (3)</u>	<u>SUERC-13124</u>	<u><math>^{14}\text{C}</math></u>	<u>14498</u>	<u>166</u>
Ballantyne et al. (2014)	Jura (4)	SNC-02	CRE	14006	1690
Ballantyne et al. (2014)	Jura (4)	SNC-03	CRE	12352	1414
<b>Ballantyne et al. (2014)</b>	<b>Jura (4)</b>	<b>SNC-06</b>	<b>CRE</b>	<b>16875</b>	<b>1102</b>
<b>Ballantyne et al. (2014)</b>	<b>Jura (4)</b>	<b>SNC-07</b>	<b>CRE</b>	<b>16819</b>	<b>1025</b>
Baltzer et al. (2010)	W coast of Scotland (5)	UL2853	$^{14}\text{C}$	16587	311
Small et al., (2013)	Mid Shelf (5)	AAR-2606	$^{14}\text{C}$	16664	279

908

909

910 Table 2. Sample information for all  $^{36}\text{Cl}$  samples from Glen Brittle and Soay.

Sample Name	Lat.	Long.	Elevation (m)	Shielding correction	Sample thickness (cm)	Lithology	Density (g/cm)
<u>Glen Brittle</u>							
BRI01	57.21595	-6.29651	10	0.9891	2.3	Basalt	2.6
BRI02	57.21652	-6.29641	11	0.9891	3.2	Basalt	2.6
BRI03	57.21667	-6.29678	10	0.9891	1.5	Basalt	2.6
BRI04	57.21602	-6.29554	11	0.9891	2.2	Basalt	2.6
<u>Isle of Soay</u>							
SOAY1	57.16073	-6.18362	13	0.9993	2.5	Gabbro	2.6
SOAY2	57.16079	-6.18352	14	0.9993	1.4	Gabbro	2.6
SOAY3	57.16118	-6.18385	15	0.9993	1.5	Gabbro	2.6
SOAY4	57.16125	-6.18392	15	0.9993	1.7	Gabbro	2.6
SOAY5	57.16120	-6.18389	9	0.9993	1.5	Gabbro	2.6
SOAY6	57.16067	-6.18340	10	0.9993	1.4	Gabbro	2.6
SOAY7	57.16076	-6.18362	15	0.9993	1.6	Gabbro	2.6

911

912

913 Table 3. Chemical and analytical data for all  $^{36}\text{Cl}$  samples. Ratios are rounded to two  
914 significant figures. Calculated concentrations reflect precision of AMS measurements.

Sample Name	Sample mass (g)	Carrier added (g)	$^{35}\text{Cl}/^{37}\text{Cl}$	Uncert. (%)	$^{36}\text{Cl}/^{35}\text{Cl}$	Uncert. (%)	$^{36}\text{Cl}/^{37}\text{Cl}$	Uncert. (%)	$^{36}\text{Cl}$ conc. (at g $^{-1}$ )	Uncert. (abs)
<u>Glen</u>										
<u>Brittle</u>										
BRI01	15.1294	0.4844	9.55E+01	0.931	5.73E-14	6.576	5.46E-12	6.548	110167	7943
BRI02	14.9876	0.4824	1.08E+02	1.216	3.81E-14	6.223	4.11E-12	6.180	70422	5140
BRI03	15.0566	0.4818	1.05E+02	0.646	5.87E-14	5.557	6.16E-12	5.509	112557	6893
BRI04	12.9649	0.4824	1.30E+02	0.692	4.55E-14	8.045	5.91E-12	8.012	98678	8902
<u>Soay</u>										
SOAY01	20.0777	0.4853	5.59E+01	0.571	6.92E-14	4.806	3.86E-12	4.751	98972	5545
SOAY02	20.0711	0.4853	1.73E+01	0.253	6.81E-14	5.188	1.18E-12	5.135	113848	6786
SOAY03	20.0162	0.4787	2.40E+01	0.345	5.70E-14	5.297	1.37E-12	5.247	86176	5447
SOAY04	20.0341	0.478	2.26E+01	0.535	3.79E-14	6.449	8.56E-13	6.408	53701	4515
SOAY05	16.8693	0.4781	2.33E+01	0.883	5.68E-14	5.147	1.32E-12	5.096	108742	6183
SOAY06	20.1048	0.4816	6.39E+00	0.276	6.34E-14	5.954	4.04E-13	5.909	179705	12009
SOAY07	19.9611	0.4818	7.73E+00	0.379	6.19E-14	5.31	4.78E-13	5.262	150704	8986

915

916

Table 4. Whole rock geochemistry of samples from Glen Brittle and Soay.

Sample Name	SiO <sub>2</sub> (wt-%)	Na <sub>2</sub> O (wt-%)	MgO (wt-%)	Al <sub>2</sub> O <sub>3</sub> (wt-%)	MnO (wt-%)	H <sub>2</sub> O (wt-%)	Sm (ppm)	Gd (ppm)	K <sub>2</sub> O (wt-%)	CaO (wt-%)	Cl (ppm)	TiO <sub>2</sub> (wt-%)	Fe <sub>2</sub> O <sub>3</sub> (wt-%)	P <sub>2</sub> O <sub>5</sub> (wt-%)	U (ppm)	Th (ppm)
<u>Glen Brittle</u>																
BRI01	46.19	1.96	8.62	13.17	0.17	2.42	2.61	3.25	0.301	12.16	2.76	1.85	13.06	0.01	0.04	0.16
BRI02	41.99	1.60	13.1	12.04	0.2	2.18	3.9	4.39	0.18	7.90	2.13	2.78	17.85	0.06	0.08	0.32
BRI03	47.64	1.99	8.52	13.68	0.16	2.01	7.26	3.09	0.18	11.97	2.25	1.77	11.98	0.02	0.04	0.15
BRI04	46.71	1.75	8.92	12.05	0.18	1.83	2.66	3.3	0.26	13.08	1.53	2.10	13.01	0.02	0.04	0.12
<u>Soay</u>																
SOAY01	45.77	0.96	11.07	20.13	0.09	0.44	0.5	0.82	0.03	14.08	4.69	0.27	7.11	0.02	0.02	0.11
SOAY02	44.55	1.03	12.49	20.96	0.09	0.41	1.30	0.69	< 0.005	12.99	23.69	0.25	7.17	0.02	< 0.01	0.03
SOAY03	44.92	1.01	13.01	22.26	0.06	0.48	0.15	0.33	< 0.005	13.16	15.14	0.1	4.97	0.01	< 0.01	0.02
SOAY04	42.94	0.07	28.02	10.14	0.13	0.62	0.28	0.5	< 0.005	7.28	16.32	0.18	10.34	0.01	0.01	0.06
SOAY05	47.12	1.58	1.88	29.28	0.04	0.56	0.56	0.87	0.02	16.46	19.06	0.34	2.74	0.02	0.02	0.10
SOAY06	47.08	1.25	5.76	23.44	0.09	1.30	0.40	0.71	0.06	15.87	109.82	0.19	4.90	0.02	< 0.01	0.01
SOAY07	48.15	0.51	12.79	8.85	0.18	1.36	1.57	2.66	0.04	15.74	77.84	0.63	11.63	0.02	< 0.01	0.02

918 Table 5. Comparison of CRE ages from Skye calculated using alternative calculation  
 919 methods and scaling schemes. Full uncertainties (analytical uncertainties). CRE ages  
 920 used in interpretation highlighted in bold text.

Calc. method	<i>Schimmelpfennig et al. (2009)</i>		<i>Marrero et al. (2016a)</i>		Marrero et al. (2016a)	
Prod. rates	<i>Marrero et al. (2016b)</i>		<i>Marrero et al. (2016b)</i>		Marrero et al. (2016b)	
Scaling	<i>Lm</i>		<i>Lm</i>		SA	
	<i>Age</i>	<i>Uncert.</i>	<i>Age</i>	<i>Uncert.</i>	<i>Age</i>	<i>Uncert.</i>
SOAY1	17.2	2.1 (1.5)	17.0	1.8 (1.5)	<b>15.0</b>	<b>1.3 (0.9)</b>
SOAY2	19.0	2.3 (1.5)	19.0	2.0 (1.5)	<b>16.4</b>	<b>1.5 (1.0)</b>
SOAY3	14.9	1.8 (1.4)	14.6	1.6 (1.4)	12.9	1.2 (0.8)
SOAY4	15.0	1.9 (1.6)	14.7	1.8 (1.6)	13.0	1.4 (1.1)
SOAY5	15.2	1.8 (1.0)	14.9	1.5 (1.0)	13.1	1.1 (0.8)
SOAY6	17.6	2.5 (1.1)	16.9	2.4 (1.1)	<b>14.8</b>	<b>1.8 (1.0)</b>
SOAY7	17.2	2.2 (0.9)	17.0	2.0 (0.9)	<b>14.6</b>	<b>1.5 (0.9)</b>
BRI01	19.0	2.4 (1.4)	20.6	2.2 (1.5)	<b>18.2</b>	<b>1.7 (1.3)</b>
BRI02	18.9	2.2 (1.4)	19.4	2.1 (1.5)	<b>17.3</b>	<b>1.6 (1.3)</b>
BRI03	21.9	2.6(1.4)	22.0	2.3 (1.4)	<b>19.4</b>	<b>1.7 (1.2)</b>
BRI04	17.3	2.1 (1.6)	17.5	2.1 (1.6)	<b>15.5</b>	<b>1.7 (1.4)</b>

921

Figure 1  
[Click here to download high resolution image](#)

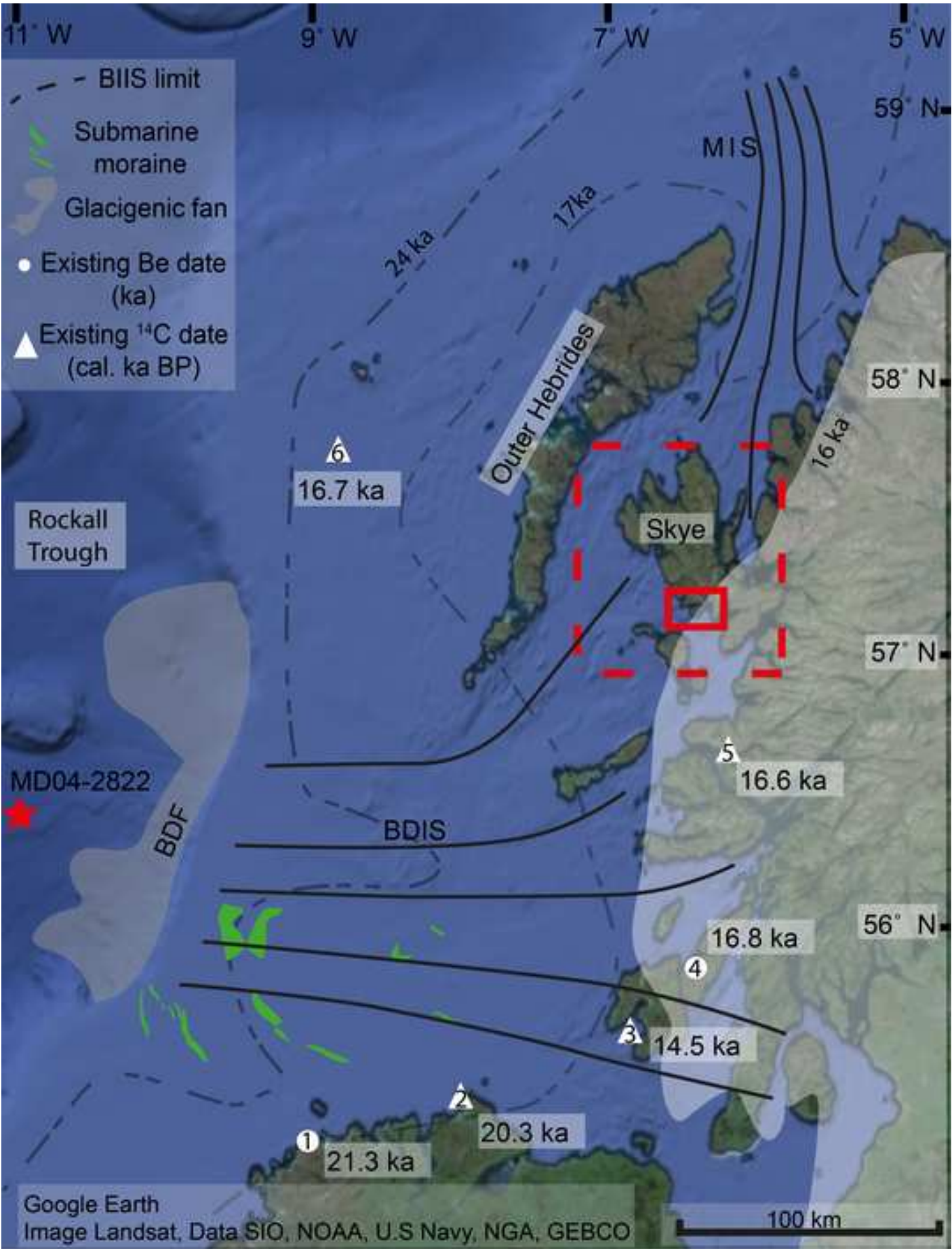




Figure 2  
[Click here to download high resolution image](#)

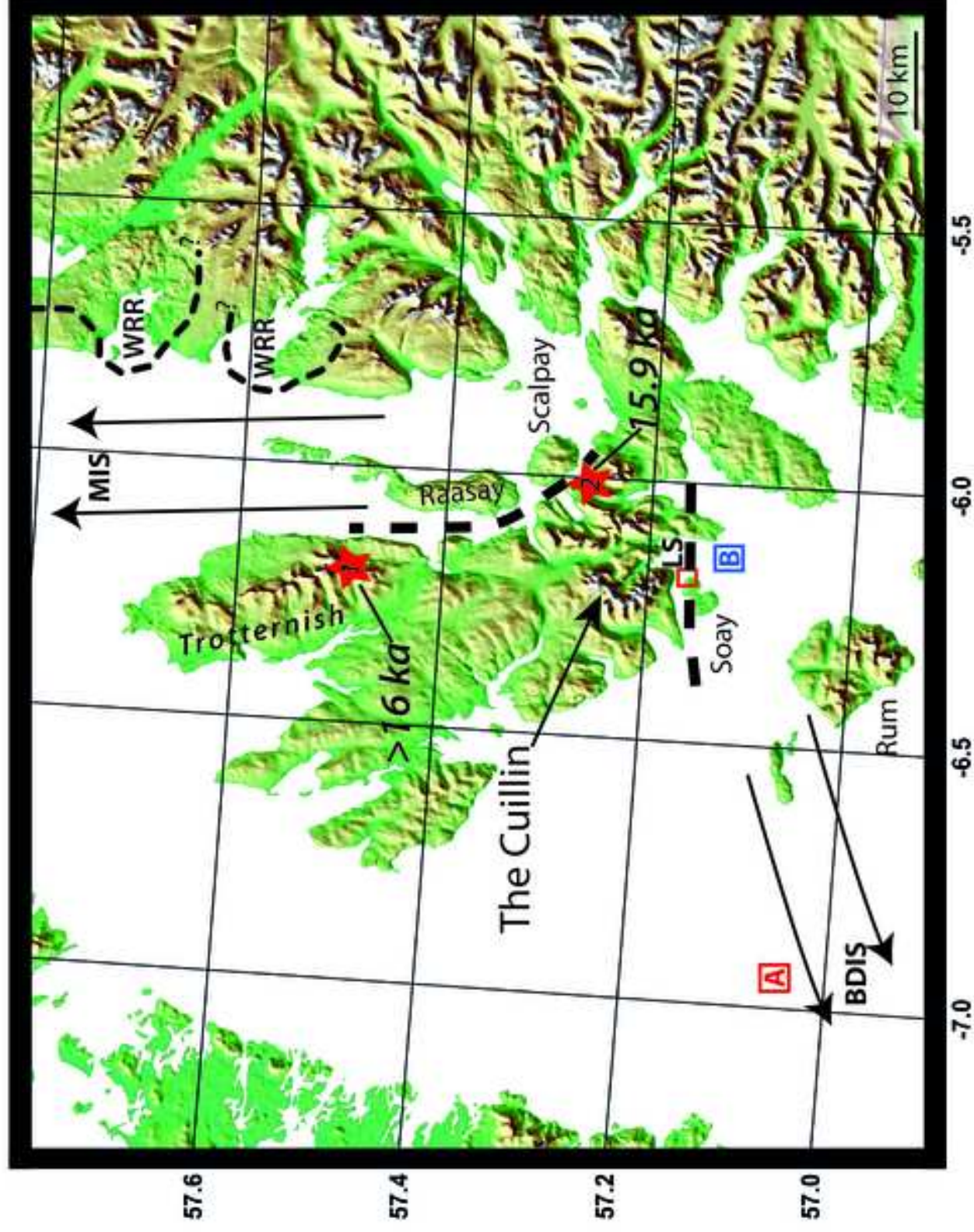


Figure 3  
[Click here to download high resolution image](#)

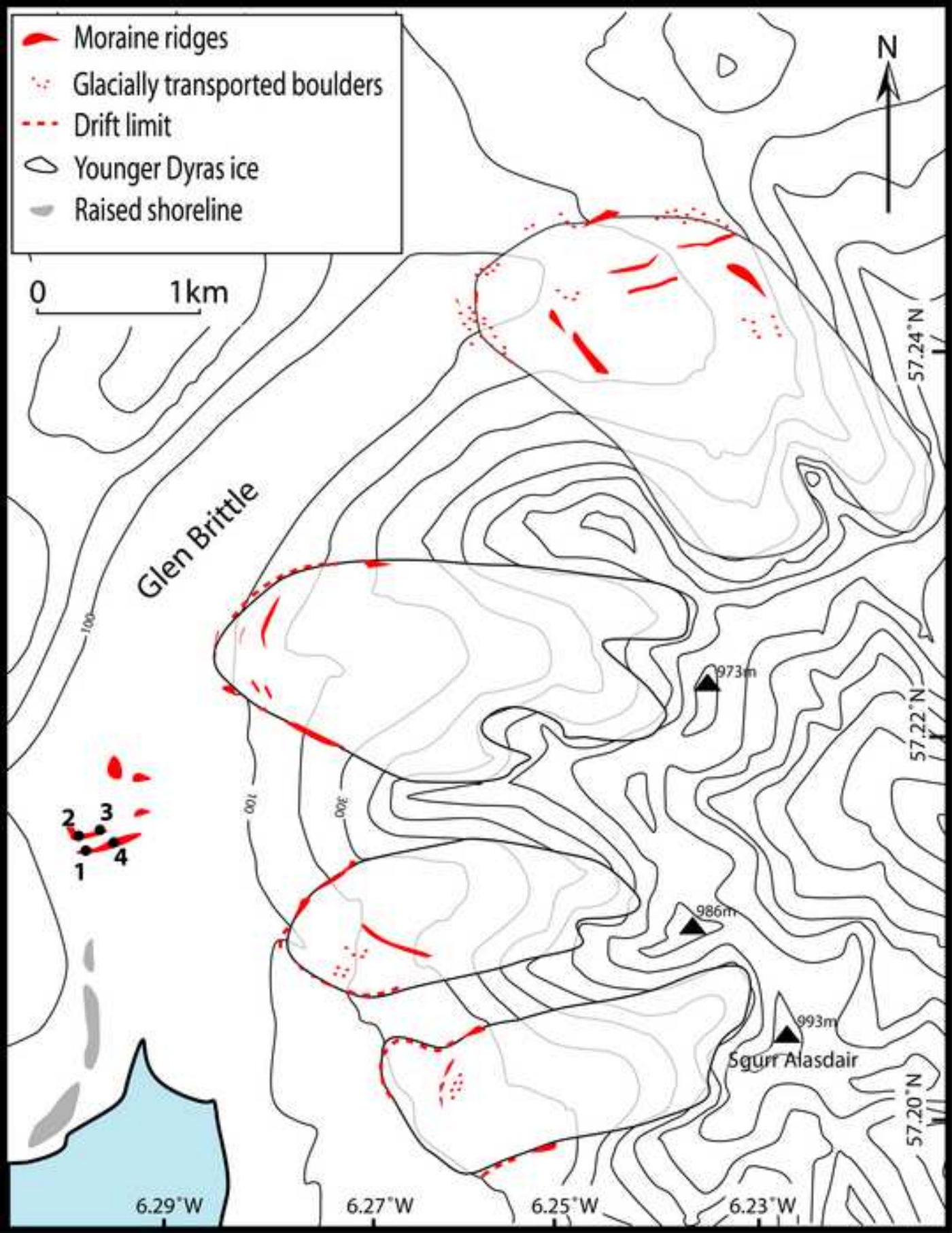




Figure 4  
[Click here to download high resolution image](#)

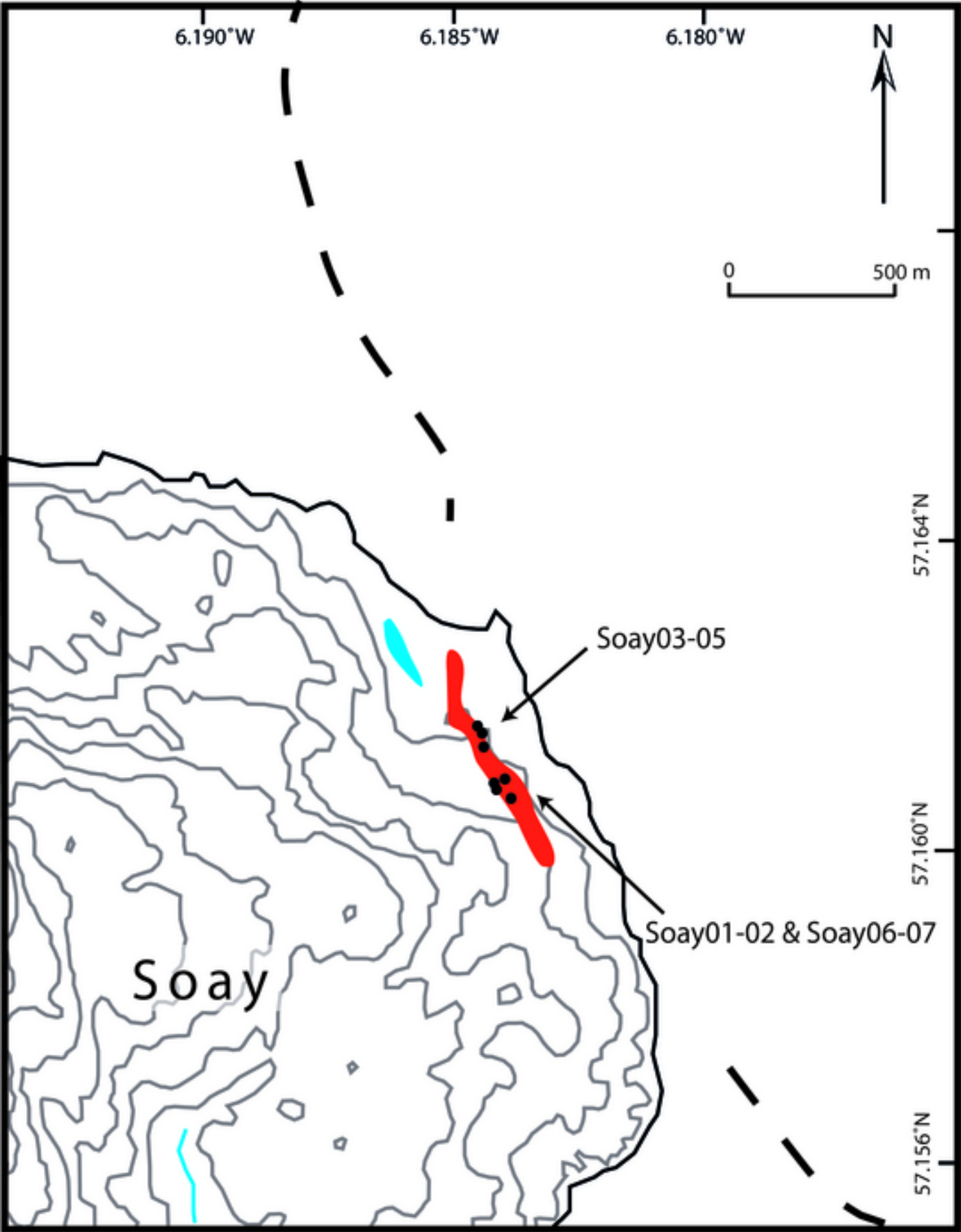


Figure 5  
[Click here to download high resolution image](#)





Figure 6  
[Click here to download high resolution image](#)





Figure 7  
[Click here to download high resolution image](#)

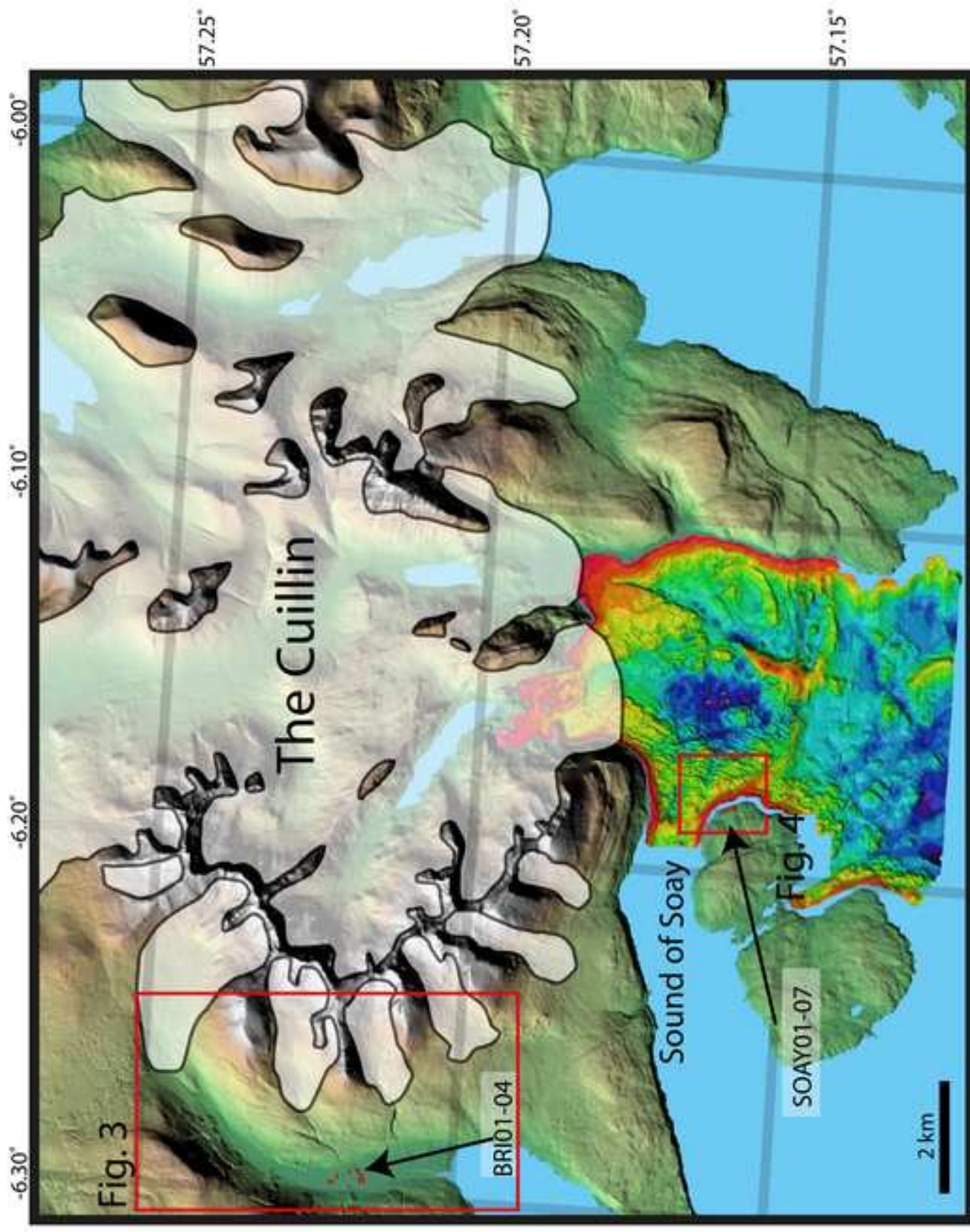




Figure 8  
[Click here to download high resolution image](#)

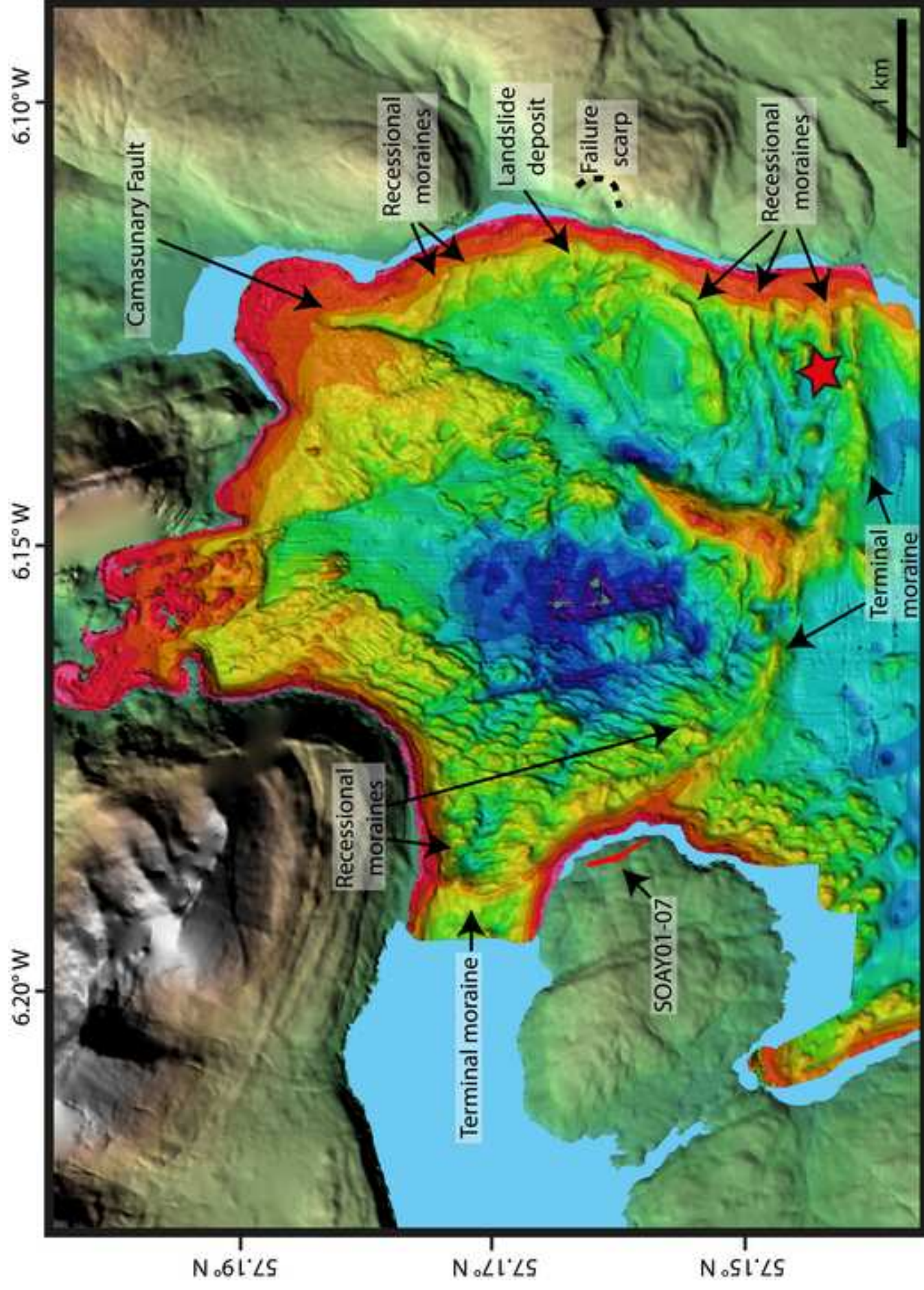


Figure 9

[Click here to download high resolution image](#)

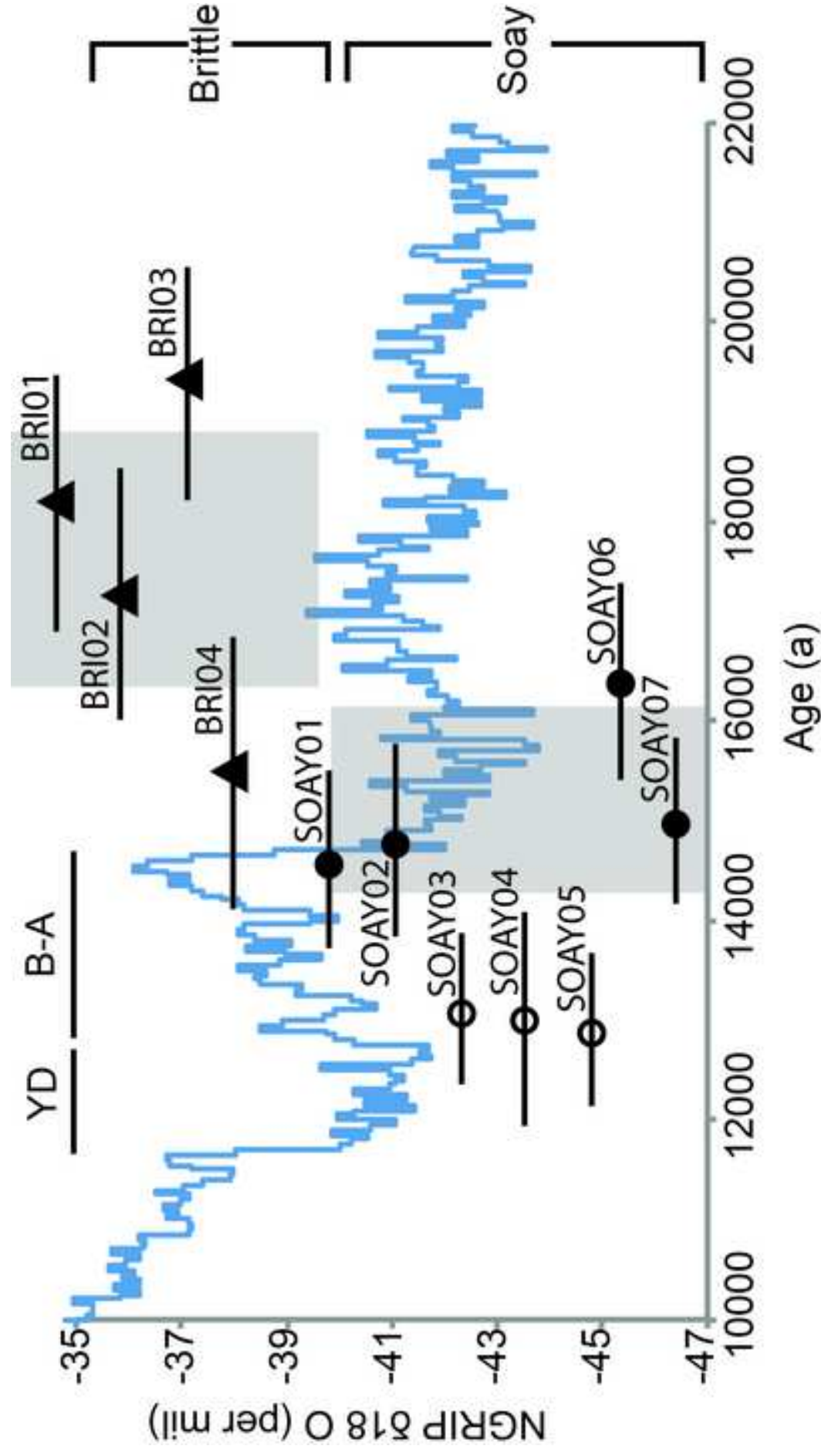




Figure 10  
[Click here to download high resolution image](#)

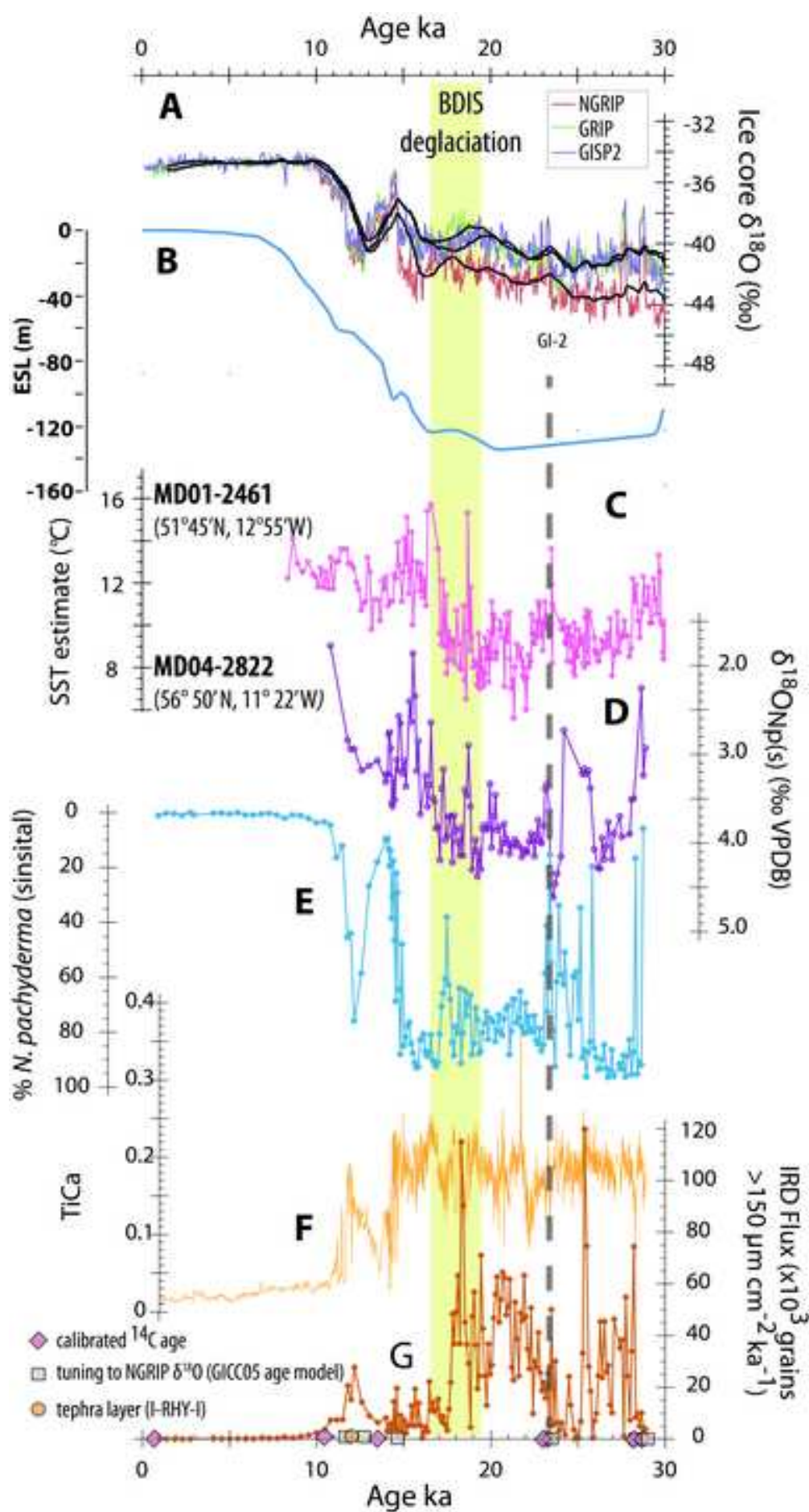
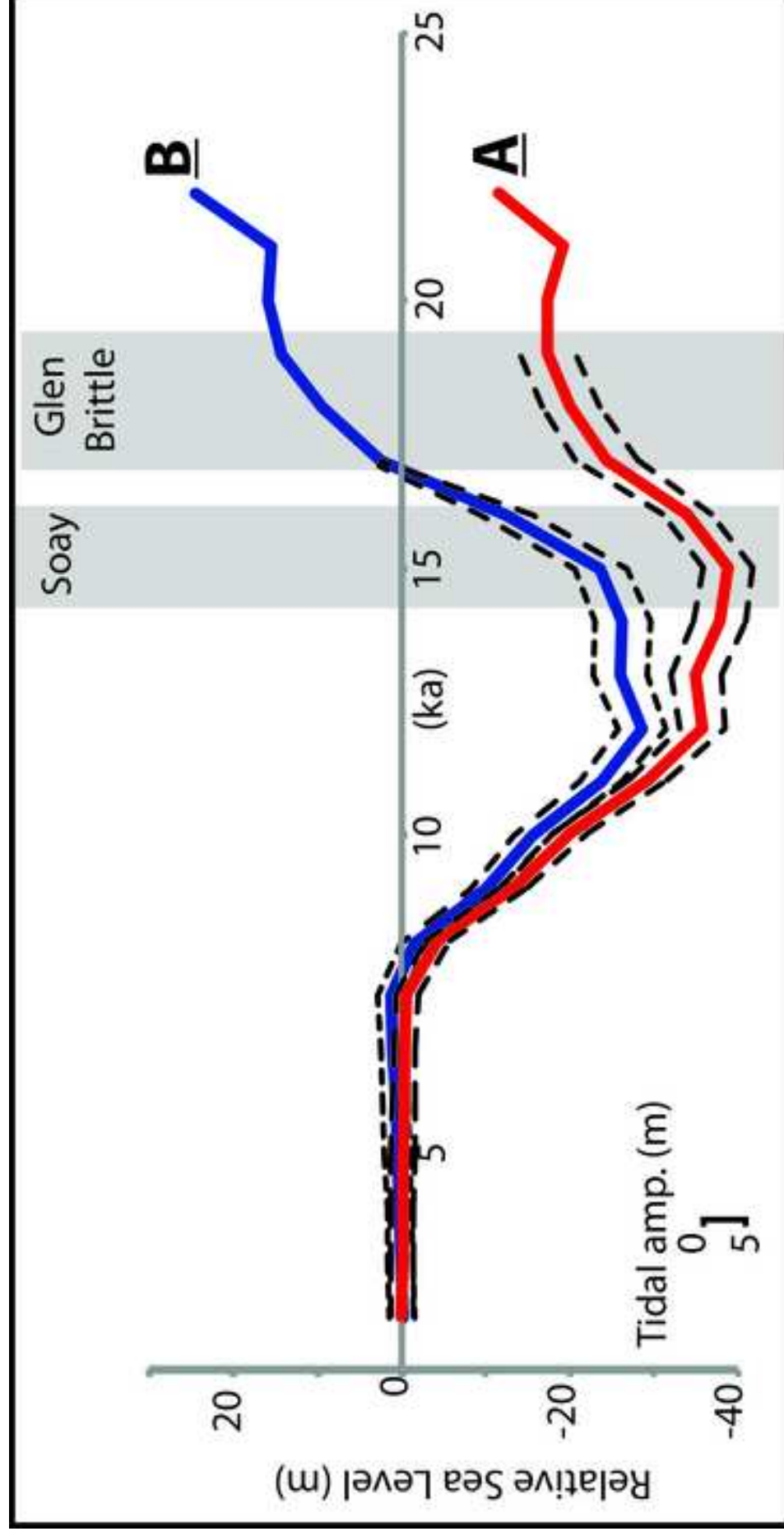


Figure 11

[Click here to download high resolution image](#)



### Highlights

- We present new  $^{36}\text{Cl}$  exposure ages from southern Skye, northwest Scotland.
- Deglaciation of a marine terminating ice stream that drained the BIIS occurred by  $17.6\pm 1.3$  ka.
- Offshore bathymetry reveals a moraine delimiting a pre-Younger Dryas readvance.
- Dated to  $15.2\pm 0.9$  ka and occurred at the same time as a regional scale readvance.

Reviewers' comments:

Reviewer #1: The paper provides an interesting review of the state of knowledge of deglaciation in the study area, and the results obtained help to improve knowledge on the subject. However, there is a need to improve the clarity of the text and figures in order to help the reader understand the real meaning of these results.

In particular, the rationale for the ages selected to explain the possible stillstand/readvance glacial stages should be improved, and the results obtained should be interpreted more cautiously when relating these stages to regional climatic phases.

I suggest the following improvements in this regard:

Abstract:

Synthesize or remove the general ideas (lines 26 -29), and instead clarify the precise objective of the study and indicate what kind of landforms were sampled and provide more precision in the location data. When describing the results, it would be useful to indicate the range of dates obtained in the datings, according to the different age calculator models applied, as well as the variety of ages obtained for different samples from the same moraine, in order to clarify the actual degree of uncertainty in the ages reported in the study. The chronological relationship between the landforms analysed in this study and recognised climatic phases in the region should be formulated as a hypothesis, not as established fact, due to the degree of uncertainty of the results. – *Abstract has been modified along these lines. There is more detail on location, specifically that the samples are from boulders on two moraines in Skye. The range of mean values for the moraines depending on choice of calculation method/scaling has been included.*

1. Introduction

The first two paragraphs discuss very general aspects (lines 44-64) which are not subsequently analysed in the discussion; they could therefore be considerably condensed. – *These paragraphs have been amalgamated into one introductory paragraph intended to set the scene as to why studying former marine ice stream provides useful information.*

There is a very interesting update of knowledge on the study area (line 83 onward), but it would be very helpful if this were preceded by a new paragraph, however brief, describing the state of knowledge on the stages of deglaciation in the western sector of the British-Irish Ice Sheet, which should then be addressed further in the discussion. I think it would be interesting to cite the data provided in the most recent synthesis papers published, such as Clark et al. (2012) and Hughes et al. (2016) and to include the latest contributions, such as Peters et al. (2016). This would help to improve the paper's focus on its actual contribution: the chronology of landforms. – *A section has been added (lines 103-109). This is after the point the reviewer suggests it be inserted however we feel that it sits better as a synthesis of the pattern of deglaciation after the existing geochronology has been introduced as it was this geochron that was used to create the isochrones We have added selected isochrones to Figure 1.*

## 2. Study site

A reader who is unfamiliar with the study area will find it difficult to locate the areas described. To remedy this, it is essential to show all geographical names on the maps (Figures 1 and 2) and to include geographical coordinates in Figure 1. – *We have added place names to Figures 1 and 2 (also suggested by Reviewer 2).*

## 3. Results

The exact location of each sample and its geomorphological meaning is not described in either the text or the figures. Neither is a description given of the geomorphology of the area sampled in the section on the study area. The existence of several moraines in the Glen Brittle sector is mentioned (line 148), but the authors do not clearly state which moraines they took samples from or what geomorphological relationship exists between them. – *Text added in methods section and samples shown on map in new figures.*

Regarding the Soay sector, the authors do not give a detailed explanation as to why the moraine studied should be interpreted as from the same unit as that observed by bathymetry (Scavaig moraine). The geomorphological relationship between the two study areas is not made clear in the text. This difficulty in comprehending the exact geomorphological context of each of the samples is accentuated by the fact that most of the samples from each sector are given exactly the same geographical coordinates. It is unclear whether this coincidence is due to error or to a lack of accuracy regarding the location. In fact, the only place in the paper where reference is made to the geomorphological characteristics of the moraines studied is in the discussion section, when it should be in the results, and the information provided is minimal (line 350 onward). – *The Soay moraine is interpreted as a continuation of the offshore moraine because it is directly traceable onto and off the island and this aligns directly with the moraine seen in the swath bathymetry. The section on the geomorphological characteristics has been moved to the results and the reasoning for interpreting the moraine section on Soay as the same feature as the Loch Scavaig moraine has been added (lines 306-310). Additional text (Line 149-153) has been added to highlight the relationship between the two study areas. The sample locations have been checked and more precision given in the table. There are new figures 3 and 4 that locate each individual sample on its respective moraine.*

To remedy this, a map or image should be included for each sample area, in which each sample is located in detail, within a specific geomorphological context, and this should also be described in sufficient detail in the text. – *Figures have been added and text updated.*

## 4. Discussion

In the previous section (results), decisions are made when selecting the ages considered as valid for each geomorphological unit. These are selected from different possible ages, according to the different scalings applied (line 308 onward) and according to the results for different samples from the same moraine (line 335 onward). However, this decision should be made in the discussion section, following further analysis. – *The selection of the ages we believe best represent the true moraine age has been moved to the discussion section*

The contrast between the results obtained with the age calculation model and the production rates of Schimmelpfenig et al. (2009, 2011 and 2014) and Marrero et al. (2016 a and b) is very interesting and

requires, if possible, a more detailed explanation. – *We have been in contact with Shasta Marrero and the difference in ages between the Lm scaling using CRONUScalc and Irene's calculator has been rectified. The age difference between the Lm and SA scaling however is real. The LSD scaling schemes (including the SA) treat Muons/Low energy Neutrons differently to the Lal based scalings and this may cause differences in <sup>36</sup>Cl ages. Additionally, we could speculate that it may be due to the elevation atmospheric pressure model used. We wish to avoid broad speculation and complexities beyond the scope of the paper. The CRONUScalc paper notes that there may be some difference between Lm and SA in some locations but our difference does seem large. However barring further analysis we are unable to comment further. We have added a line in the results section acknowledging the age difference is currently enigmatic.*

The same is true when assessing the criterion used to establish the ages of some blocks as valid and reject others. For example, in the Soay sector, it is not clear why the authors only considered the age of the oldest samples to be valid (SOAY 1 and 2), although the other three (SOAY 3, 4 and 5) shared a common age. On the one hand, the authors should explain why a possible exhumation of those blocks occurred precisely at the same time, and on the other, they should also explain why, if some blocks were exhumed, others were not in an earlier period. – *We have added additional text outlining why we believe contemporaneous exhumation of the three younger samples is possible (Lines 397-406).*

In addition, if the impossibility of cosmogenic inheritance in Soay samples is accepted, it is not clear why this criterion is not applied to the Glen Brittle sector, where the age of the oldest samples (BRIO 1 and 3) does not serve to explain an advance with this age, as in Soay, but rather the arithmetic mean age is selected between samples from the same sector. Although the solution adopted in the selection of valid ages is one option, it is not the only one, and it should therefore be carefully discussed and clarified. – *We acknowledge that our ages may over or under estimate the age of the Glen Brittle moraine. For Soay we base our interpretation on geomorphic evidence (new lines 417-428; i.e. boulder height, spatial proximity of young samples) and evidence from elsewhere in Scotland that does not favour ice survival through the warm interstadial which would be required if the young Soay ages were the true moraine age.*

As mentioned earlier, the lack of a concrete explanation of the geomorphological context of the samples leaves the reader with many unanswered questions.

The rest of the discussion proceeds as if there were total certainty about the absolute precision of the ages selected as valid. This allows the authors to relate the moraines studied to recognised climatic events in the region. In my opinion, they should be more cautious, leaving the possibility of a wider range of ages open in the discussion, and differentiating in each statement between certainty and what are actually their hypotheses. This difference is made clear in the conclusions, but as already indicated, not in the abstract. – *We have amended the discussion in various places to highlight the uncertainty in our ages and added an additional paragraph (lines 429-435) explicitly stating this and that we are proposing a hypothesis.*

CITED REFERENCES: Hughes, A. L. C., Gyllencreutz, R., Lohne, Ø. S., Mangerud, J., Svendsen, J. I. 2016. The last Eurasian ice sheets - a chronological database and time-slice reconstruction, DATED-1. Boreas, Vol. 45, pp. 1-45.

Peters et al., 2016. Sedimentology and chronology of the advance and retreat of the last British-Irish Ice Sheet on the continental shelf west of Ireland, Quaternary Science Reviews 140 101-124.



Reviewer # 2:

In this paper the authors discuss the timing of possible past ice extent variations on the Isle of Skye during the Lateglacial based on 11  $^{36}\text{Cl}$  exposure ages. The paper is well written and interesting to read as it interweaves published data and hypotheses on the timing of ice margin variations.

I think the paper has the potential to be significant, nevertheless the following two deficiencies must be addressed before this paper is publishable:

1. The maps are rather insufficient: a map showing the specific geomorphology of the dated sites is required; a map showing regional relationships would increase the clarity of the presentation.
2. The calculation of the  $^{36}\text{Cl}$  ages must be checked again.

These two topics will be discussed in more detail below in addition to further minor suggestions.

I believe this paper could have an important impact on our understanding of glacier variations in western Scotland during the Lateglacial. It is a nice summary although the presentation is rather ineffective and could be quite easily improved.

Unfortunately the cosmogenic data is not portrayed in a way useful to the reader. Actually I have no idea which boulders are where with respect to the moraines (etc.). The photos are somehow ok but do not allow an understanding of what was dated with respect to the landforms, former ice margins etc. Perhaps I have missed a figure? Every dated boulder and the associated landforms must be shown on a map. –*New Figures have been added that show the location of the boulders with respect to the moraines. (i.e. taken from the moraine crest)*

This paper is written as if everyone is an expert in UK geography. I do not think it is appropriate to expect the reader to look up terms in google maps to figure out what the authors are talking about.

Simply labeling the existing figures better could rectify much of this.

The following locations are discussed but not identified on maps:

Inner Hebrides - *Removed*

outer Hebridean platform (where is the boundary between these two?) –*Boundary is concurrent with western shoreline of Outer Hebrides. Text amended and Outer Hebrides labeled on Figure 1.*

St Kilda basin – *Changed to “mid-shelf”*

Sea of the Hebrides – *removed from text*

Sound of Soa – *Labeled in Figure 5.*

Rum- *Labeled in Figure 2*

Cuillin This is referred to several times, seems to be a key location. Where is it? Just put it on a map.

*Cuillin is the name of the mountains of Skye. It is Labeled on Figure 2 and Figure 5*

Coruisk basin/Scavaig basin – *Coruisk removed from text, Scavaig basin changed to Loch Scavaig*

Loch Scavaig - *Labeled in Figure 2.*

Barra Fan – *Should read Barra-Donegal Fan, changed and shown on figure 1.*

Rockall Trough – *Added to figure 1.*

Location of core MD01 2461, which figure? – *It is not possible to show this core without a dedicated figure. We give its co-ordinates and describe its distance and direction from the study area.*

## Study Site

Where is the map that goes with this? Must the reader go find the maps in Walker or Ballantyne? The long-term impact of this paper would definitely increase if the previously dated landforms are shown on a map in relation to the landforms dated in this paper, and of course with respect to postulated former ice margins. – *Added location of Strollamus moraine to Figure 5 (both sites are already shown on figure 2). Walker et al., did not present a map of the moraines in Glen Brittle (the ones that are dated in this paper). We present a new Figure, Figure 3, a larger scale map of Glen Brittle showing the moraines, sampled boulders and relationship to the Younger Dryas limits mapped by Ballantyne. Figure 4 is a very large scale map of the northeast corner of Soay showing trace of the offshore moraine, onshore segment and sample locations.*

## <sup>36</sup>Cl methods

BaNO<sub>3</sub>? Actually it is Ba(NO<sub>3</sub>)<sub>2</sub> – *Changed.*

What value is used for Po in the age calculation? Please state this. This number is required so that in the future, we can know exactly how the ages were calculated. – *Value has been added. We apologise for the accidental omission.*

The supplementary data tables are incorrectly labeled. CaO, K<sub>2</sub>O are target elements not non-target elements. In any case the elemental data should be combined in one table and should be included in the main paper, not as a supplemental table. All data required to calculate an age must be in the main body of the paper for future recalculations. – *Tables have been combined and included in main body of paper*

It may be irrelevant to use the Schimmelpfennig et al. (2009) production rates. – *The column has been removed from the table*

Actually, I am not sure why there should be such huge differences between the results from the other three calculation methods (last three columns in Table 3). The equations and constants are well known. In detail the calculation methods should be generally the same. Effects due to scaling at this latitude and altitude should not be so great. These numbers need to be carefully checked again. – *We have contacted Shasta Marrero. The discrepancy between the ages as calculated using the Lm scaling using Schimmelpfennig et al. (2009) and Marrero et al (2016a) has been rectified, this was due to a error in the spreadsheet we were using. The difference between Lm and SA scaling is however real as they use the same input data into CRONUScalc (bar the scaling scheme chosen). We could speculate*



that this may be due to the elevation atmospheric pressure model used but this ventures into idle speculation and complexities beyond the scope of the paper. The CRONUScalc paper notes that there may be some difference between Lm and SA in some locations but our difference does seem large. However barring further analysis we are unable to comment further. We have added a line in the results section acknowledging the age difference is currently enigmatic. Again we have discussed this with Shasta who acknowledges that this difference is larger than one might expect but currently the cause in this specific location is not known.

## DISCUSSION

Line 323: "The boulder ages are not a single population." This based on statistical treatment. How do the ages look spatially? At this moment the reader has no idea where the boulders are located in space with respect to the landform(s?). Maybe there is some spatial geomorphological relationship between the group of old ages and group of young ages for the SOAY samples. I appreciate that the authors considered this, but the reader should be able to assess the situations himself. – *Text has been added (lines 378-389) to discuss the potential spatial relationship*

328: "...generally cosmogenic moraine ages can underestimate...." This is strictly only true for  $^{10}\text{Be}$  ages. The data set of Heyman is made up of  $^{10}\text{Be}$  ages. It is well known that because of the stronger depth penetration and higher percentage of production due to muons that  $^{36}\text{Cl}$  may have (much) more inheritance than  $^{10}\text{Be}$ .

Similarly, the response of the  $^{36}\text{Cl}$  age to erosion (which always makes  $^{10}\text{Be}$  ages older) is less predictable than for  $^{10}\text{Be}$ . Indeed erosion/spalling can make  $^{36}\text{Cl}$  ages apparently older. The  $^{36}\text{Cl}$  specific issues should be discussed. – *The  $^{36}\text{Cl}$  specific issues are mentioned (374-381). We sampled as best we could to avoid inheritance and/or boulder spalling (outlined in text added to methods section) but this is obviously not infallible. We acknowledge the possibility that our ages may overestimate moraine age.*

329: This is true, it is generally unlikely that inheritance would yield a 'pattern'.

335: The location of the core with respect to the ice limit is not shown. Why should an age of 13 ka not agree with deglaciation at 12.8 ka? Please elaborate. – *Reference to the radiocarbon age has been removed.*

372: What/where is the Strollamus moraine? What is the Scavaig moraine? Why is it a medial moraine? Where are all these moraines located? – *The Strollamus moraine is shown on Figure 2 and Figure 5. We explicitly mention it in the captions to these figures so we hope that it is clear where it is located. Its interpretation as a medial moraine is discussed fairly extensively in Benn 1990 and Small et al., 2012. In reference to the Scavaig moraine, it is not a medial moraine. We have found a typo in the text (line 388) where 'Scavaig' should read Strollamus.*

## FIGURES

Fig. 1. Please identify the sites with respect to Table 1. – *Sites have been numbered as in an amended*

### Table 1.

Fig. 2. Map with previous studies, red stars. Please identify which site is which. – *Stars are now numbered*

Fig. 3. Why are the moraines and boulders shown in the photos not located in detail on any maps? *New Figures (Figures 3 and 4 show the location of the boulders)*

Figure 3A. ".two parallel moraine ridges.." where are these on Fig. 5 or 6? *See Figure 3, the ridges were already depicted on Figure 5 (now 7) although the scale may not be ideal hence the higher scale Figure 3.*

Fig. 7. Use a different symbol for each site. Identify each boulder (add to plot labels BRI01 etc.) as they are shown on the (now non-existent) geomorphological boulder/landform map and listed in the tables. – *Labels have been added and symbols changed.*

## TABLES

Table 1. These sites need to be directly connected to the figures. N. Donegal coast, I say these locations must be shown on a map. Note there are numerous ages listed in Table 1 for each site of the previous work. Did you take a mean for each site? Please specify. Again how do the ages in the table specifically relate to Figure 1? – *Caption amended to indicate that it is the mean of the CRE ages included in Figure 1. Similarly it now explains that it is the oldest  $^{14}\text{C}$  age from a site that is shown.*

Table 3. The  $^{36}\text{Cl}/^{37}\text{Cl}$  ratio uncertainties should match the significant figures on the ratio.

The significant figures on the  $^{36}\text{Cl}$  concentrations are overestimated. They should as well match those of the measured  $^{36}\text{Cl}/^{37}\text{Cl}$  ratio:  $11.01 \times 10^4$  uncertainty:  $0.79 \times 10^4$  etc. The precision of the atoms cannot exceed the precision of the AMS measurement. – *The ratios are rounded otherwise the table gets very wide and unwieldy. The concentrations are calculated from the AMS data and match the precision in this. We have added to the caption to highlight this.*

**Supplementary Data**

[Click here to download Supplementary Data: Supp Tab1.xlsx](#)